A subpool of the large subunit of ribulose bisphosphate carboxylase-oxygenase has a dual function in oxidative stress tolerance in *Chlamydomonas reinhardtii*

Jamieson Dhaliwal

A Thesis
in
The Department
of
Biology

Presented in Partial Fulfilment of the Requirements
for the Degree of Masters of Science (Biology) at
Concordia University
Montreal, Quebec, Canada

August 2013

CONCORDIA UNIVERSITY

School of Graduate Studies

This is to certify that the thesis prepared

By: Jamieson Dhaliwal

Entitled: A subpool of the large subunit of ribulose bisphosphate carboxylase-oxygenase has a dual function in oxidative stress tolerance in *Chlamydomonas reinhardtii*

And submitted in partial fulfillment of the requirements for the degree of

Master of Science (Biology)

Complies with the regulations of the University and meets the accepted standards with respect to originality and quality.
Signed by the final examining committee:

_____Chair
Dr. Vincent Martin

_____Examiner
Dr. Patrick Gulick

_____Examiner
Dr. Vladimir Titorenko

_____External Examiner
Dr. Malcolm Whiteway

_____Supervisor
Dr. William Zerges

Approved by _____
Graduate Program Director - Dr. Selvadurai Dayanandan

_____2013 _____
Interim Dean of Faculty - Joanne Locke

Abstract

A subpool of the large subunit of ribulose bisphosphate carboxylase-oxygenase has a dual function in oxidative stress tolerance in *Chlamydomonas reinhardtii*

Jamieson Dhaliwal

Stress granules (SGs) are cytoplasmic foci of mRNA and protein that form in eukaryotic cells during stress-induced translational arrest. Similar structures called chloroplast stress granules (cpSGs) are found in the chloroplast stroma of *Chlamydomonas reinhardtii.* Unique to cpSGs is the presence of a photosynthesis protein, the large subunit of Rubisco (RBCL). It was found that an RBCL-deficient mutant of *Chlamydomonas* has impaired oxidative stress tolerance, while a mutant that retains RBCL in the absence of the Rubisco holoenzyme has improved oxidative stress tolerance. Through genetic analyses, I show that these opposing effects are RBCL-dependant, demonstrating a dual function for RBCL in controlling oxidative stress tolerance. I then provide evidence, through biochemical analyses, for the existence of a subpool of RBCL that carries out this dual function independently of Rubisco enzymatic activities. This RBCL subpool is found to have altered properties from that of Rubisco, which may be consistent with its recruitment to cpSGs. Because the oxidation of specific biological molecules is thought to contribute to cell death during oxidative stress, I then explore a function of RBCL in controlling molecular oxidative damage. I show that RBCL is not required for the prevention of oxidative damage to protein. This result supports the finding that RBCL is able to prevent the acuumulation of oxidized RNA. Though specific to RBCL, these findings may reflect functions of cpSGs and even SGs.

Acknowledgments

I would first like to greatly thank my supervisor, Dr. Zerges, for his support, guidance, good humour, and patience throughout each stage of my studies. I would like to thank my committee members, Dr. Gulick and Dr. Titorenko, for their helpful comments and suggestions during the course of my research. I would also like to thank the members of the Zerges lab, past and present, for their assistance and companionship. In particular, Dr. James Uniacke, who initiated this project, and Yu Zhan, whom I worked alongside, and whose knowledge and skill were of great help. Finally, I would like to thank my friends and family for their encouragement, support, and understanding during these past years.

Table of contents

List of Abbreviations

ROS	Reactive Oxygen Species
RBCL	Rubisco Large Subunit
RBCS	Rubisco Small Subunit
SG	Stress Granule
cpSG	Chloroplast Stress Granule
RBP	RNA Binding Protein
RNP	Ribonucleoprotein
RRM	RNA Recognition Motif
CTM	Chloroplast Translation Membrane
8-oxoG	8-oxo-7,8-dihydroguanosine
H_2O_2	Hydrogen peroxide
O_2^-	Superoxide Anion
$OH^·$	Hydroxyl Radical
$^1O_2$	Singlet Oxygen

List of Figures

Chapter 1: Introduction

Oxidative stress and ROS production in photosynthetic organisms

Oxidative stress is a condition that results from an imbalance in the redox homeostasis of the cellular environment during which reactive oxygen species (ROS) are produced in excess of an organism or cell's capacity to detoxify them through its antioxidant mechanisms. All organisms are affected by oxidative stress, particularly aerobic organisms. An unavoidable consequence of the electron transfer reactions housed in energy transducing organelles such as peroxisomes, mitochondria, and chloroplasts, is the production of potentially hazardous highly reactive molecules such as ROS. These molecules are formed when redox reactions produce partially reduced forms of oxygen, such as hydrogen peroxide (H_2O_2), superoxide (O_2^-), or hydroxyl radicals ($OH^\cdot$); or when oxygen absorbs excess excitation energy, such as singlet oxygen ($^1O_2$) (Foyer and Noctor, 2009).

During oxygenic photosynthesis light energy is used to drive the oxidation of water, channelling its electrons through a photosynthetic electron transport chain towards $NADP^+$ to form NADPH for use in the Calvin cycle. In doing so, molecular oxygen is produced as a by-product and a proton gradient is generated across the thylakoid membrane which can be used to produce ATP. When light intensity is in excess of the chloroplast's ability to utilize it by transferring electrons to CO_2, overreduction of the electron acceptors in the photosynthetic electron transport chain occurs (Takahashi and Murata, 2008). High light and other environmental stresses therefore compromise the ability of the photosynthetic machinery and the Calvin cycle to efficiently harness light

energy and fix CO_2, respectively. These conditions lead to the potential for ROS production at several positions throughout the photosynthetic electron transport chain (Foyer and Shigeoka, 2011).

The Light harvesting complexes housed in the thylakoid membranes of chloroplasts use chlorophyll to channel excitation energy derived from photons towards the reaction centers of photosystem II and photosystem I. Chlorophyll and other tetrapyrroles, as well as the intermediates in their synthesis are potent photosensitizers, leading to ROS production when excited by light (Apel and Hirt, 2004). As such, the balance between their production and detoxification must be precisely controlled. While the mature form of chlorophyll is typically bound to protein to control its excitation, its precursors are more freely able to absorb light and produce ROS (Meskauskiene et al., 2001). Even when housed in protein complexes however, chlorophyll has the potential to produce ROS. Excited chlorophyll P680 ($P680^*$) bound by the D1 protein in the reaction center of photosystem II normally transfers a high-energy electron to plastoquinones in the thylakoid membrane. When the plastoquinone pool is overreduced during high-light intensity, the lifetime of $P680^*$ is prolonged, allowing it to react with oxygen to produce $^1O_2$ (Fischer et al., 2013). This excited form of oxygen can react with the closely packed polyunsaturated lipids of the thylakoid membranes to produce lipid peroxides (Girotti and Kriska, 2004). These in turn may react with other lipids, accelerating a chain reaction of further lipid peroxidation, which can compromise thylakoid membrane integrity (Ledford and Niyogi, 2005). In addition, $^1O_2$ and lipid peroxides can damage the D1 protein of the photosystem II reaction center, which also limits the transfer of electrons from $P680^*$ to plastoquinone, leading to further $^1O_2$ production. D1 is continually being repaired to

optimize light utilization, however in extreme cases light-induced D1 damage can lead to a reduction in photosynthetic rate, a condition called photoinhibition (Murata et al., 2007). Inhibition of photosystem I, and consequent over-reduction of the photosynthetic electron transport chain can lead to the formation of O_2^-, which is rapidly converted to H_2O_2 by superoxide dismutase (Rochaix, 2011). While H_2O_2 is relatively stable, its reaction with metal ions such as Fe^{2+} can lead to the formation of OH^-, through Fenton chemistry (Kehrer, 2000). OH^- is a highly reactive and toxic molecule and it is believed that the damaging effects of O_2^- and H_2O_2 are due to their potential for its production (Foyer and Noctor, 2009; Imlay and Linn, 1988). Many of the proteins that act as electron carriers in the photosynthetic machinery make use of Fe^{2+} as a metal cofactor, thus ROS production in chloroplasts is a constant process that must be managed to avoid the detrimental effects of oxidative stress.

Because photosynthesis is a major source of ROS, photosynthetic organisms and chloroplasts must be particularly adept at maintaining redox balance. In order to cope with the effects of ROS production, numerous antioxidant defense strategies have evolved that serve to limit the generation and diffusion of ROS, repair the damage caused by them, or replace damaged cellular components. Non-photochemical quenching is an antioxidant defense mechanism in which excess excitation energy absorbed by chlorophyll molecules in the light-harvesting complexes is dissipated as thermal energy (Holt et al., 2004). In order to prevent the transfer of excitation energy from triplet-excited chlorophyll to oxygen and the formation of $^1O_2$, the excess energy is enzymatically transferred to lipid-soluble antioxidants in the thylakoid membrane such as carotenoids and tocopherols (Li et al., 2012). In this way, non-photochemical quenching

is a protective process that limits the severity of photoinhibition. Although sustained photoinhibition itself is a negative consequence of excess energy absorption, it can also be considered as a defense mechanism. Plants and algae can limit light absorption by changing the physical orientation of leaves and chloroplasts, or by reducing the size of the light-harvesting complexes (Escoubas et al., 1995; Kasahara et al., 2002). These responses come at the expense of photosynthetic rate, but serve to reduce ROS production. Another protective mechanism used by chloroplasts to dissipate excess excitation energy is the use of alternate electron sinks. For example, when light intensity is too high to be used for the reduction of $NADP^+$ to NADPH, electrons can diverted to form H_2O in a series of reactions called the water-water cycle (Asada, 2000). In this process, O_2 is partially reduced by ferrodoxin at photosystem I, forming O_2^-. Superoxide dismutase then rapidly converts O_2^- to H_2O_2, which is then scavenged by catalase to form H_2O. Finally, a plethora of enzymatic and small molecule antioxidants exist in the chloroplast to dissipate excess excitation energy. Ascorbic acid and glutathione are two water-soluble antioxidants that scavenge ROS generated from the photosynthetic machinery in a series of reactions catalyzed by enzymes such as ascorbate peroxidase, glutathione reductase, glutathione peroxidase, peroxiredoxin, and several others (Foyer and Noctor, 2009).

Oxidative damage to biological molecules

As highly reactive intermediates with the ability to oxidize biological molecules in order to balance their unpaired electrons or, in the case of $^1O_2$, to dissipate its excess excitation energy, ROS can cause damage to the macromolecules of a cell (i.e. proteins,

lipids, DNA, and RNA) (Gill and Tuteja, 2010). Oxidative damage to these molecules has been implicated in many diseases in humans and is also thought to form the basis for cell death, growth retardation, and other adverse effects of ROS in plants. However, the relative degrees to which cell death is caused by the detrimental effects of oxidative damage versus the signaling of programmed cell death by ROS is a matter of intense debate and research attention (Foyer and Shigeoka, 2011). As mentioned above, $^1O_2$ and excited chlorophyll can cause peroxidation of the lipids in biological membranes. This can lead to decreased fluidity, leakage, and inactivation of membrane proteins, all of which compromise membrane function and integrity (Garg and Manchanda, 2009). Proteins can also be oxidatively modified in various ways. Some oxidative modifications are reversible and may serve roles in redox signalling, while others are irreversible and can lead to loss of function, misfolding and aggregation, and degradation (Ghezzi and Bonetto, 2003). One such irreversible oxidative modification is protein carbonylation. Carbonylation can occur at various sites in a protein, either by direct oxidation from ROS or by reacting with the oxidation products of other biological molecules (Stadtman and Berlett, 1997). In addition to chemical damage and ionizing or ultraviolet irradiation, DNA is susceptible to oxidative damage. One of the most commonly identified forms of oxidative modification to DNA is the formation of 8-oxoguanine (8-oxoG). Oxidative DNA damage can lead to genotoxic stress, resulting in errors in gene expression, DNA replication, and genome stability (Tuteja et al., 2009). Indeed, one reason for organellar gene transfer and genomic compartmentalization in the nucleus may be to distance DNA from the potentially dangerous redox reactions of the energy-transducing organelles (Allen and Raven, 1996).

Like DNA, RNA is also susceptible to oxidative damage. RNA is likely more easily oxidized than DNA for several reasons: it is often single-stranded, is less associated with protein than DNA, and is widely dispersed throughout the cell, often in close proximity to areas of ROS generation (Li et al., 2006). Like in DNA, 8-oxoG is the most commonly identified oxidized base in RNA, and it is used as a marker of oxidative damage (Park et al., 1992). There are several consequences of oxidative RNA damage. mRNA damage can lead to reduced protein expression, or to the expression of truncated or misfolded proteins (Tanaka et al., 2007). rRNA damage can similarly affect translation by impairment of ribosome function (Honda et al., 2005). There is also increasing evidence that oxidative RNA damage is related to numerous pathologies in humans, particularly in neurodegenerative disorders, where 8-oxoG levels in brain tissue is elevated (Nunomura et al., 2006).

In contrast to the known mechanisms for the prevention, repair, or degradation of oxidatively damaged DNA, less is known about the handling of oxidized RNA. There is evidence of a mechanism for the turnover of damaged RNA because 8-oxoG levels decreased within a few hours during recovery from stress in cultured human lung epithelial cells (Hofer et al., 2005). In addition, there are some proteins that are known to bind specifically to oxidized RNA. For example, the human YB-1 protein, which was initially identified as a transcription factor, is able to bind to 8-oxoG-containing mRNA and provide resistance to oxidative stress when overexpressed in *E. coli* (Hayakawa et al., 2002). Polynucleotide phosphorylase (PNPase), a 3'-5' exoribonuclease, also binds specifically to 8-oxoG-containing RNA (Hayakawa et al., 2001). It was found that PNPase-deficient *E. coli* cells were hypersensitive to oxidative stress (Wu et al., 2009). It

was also seen that overexpression of human PNPase in HeLa cells resulted in increased viability and reduced 8-oxoG RNA during oxidative stress (Wu and Li, 2008). While the mechanisms by which cells handle oxidized RNA are still being uncovered, it is increasingly understood that the control of damage to RNA is critical for stress response.

Stress granules

During the general arrest of translation that occurs during various stresses, mRNA released from dissociating polysomes are sequestered, along with many specific RNA binding proteins (RBPs), into large cytoplasmic aggregates called stress granules (SGs) (Kedersha et al., 1999). These microscopically visible messenger ribonucleoprotein (mRNP) structures are believed to have some functional role in cellular stress responses for several reasons: they have been identified in all eukaryotic cell types examined thus far; their formation and composition are both dynamic and reversible; when their formation is blocked prior to stress, cell survival is typically reduced (Buchan and Parker, 2009). While it has been suggested that SGs function in the reprogramming of translation and sorting of untranslated mRNAs during stress, the specific function of SGs has yet to be demonstrated. One possibility that has been suggested is that SGs form in order to control oxidative damage to RNA (Wurtmann and Wolin, 2009).

SG-like structures were first described in plant cells, where the reversible formation of protein and mRNA aggregates was observed by electron microscopy in heat-shocked tomato cell-suspension cultures (Nover et al., 1983, 1989). It was later found that these structures are distinct from the now accepted definition of SGs, by virtue of their recruitment of various heat-shock proteins, and the absence of the small ribosomal

subunit (Weber et al., 2008). Nonetheless, they provided the first suggestion that stress-induced translational arrest results in the sequestration of untranslated mRNAs into granules. Canonical SGs were later described in mammalian cell cultures exposed to heat shock or arsenite-induced oxidative stress (Kedersha et al., 2002, 1999; Kimball et al., 2003). These are defined as aggregates of poly(A)+ mRNA, and 40S ribosomal subunits along with the various translation initiation factors (eIF2, eIF3, eIF4A, eIF4E, eIF4F, eIF4G, poly(A) binding protein (PABP-1)) that comprise the 48S pre-initiation complex. In addition, an increasing number of proteins with functions in various cell processes are now known to be recruited to them. These include components of the translational-silencing machinery, RNA binding proteins (RBPs) involved in RNA metabolism (such as splicing and RNA editing), and components of stress-induced apoptotic signalling pathways (Anderson and Kedersha, 2008). Following their discovery in mammalian cells, canonical SGs have also been identified in yeast and plant cells (Hoyle et al., 2007) (Weber et al., 2008).

The steps involved in SG formation have been well studied. The first requirements are the disassembly of translating polysomes and ribosomal run-off that occur when translation initiation is blocked. This results in the availability of the core SG component: a stalled 48S pre-initiation complex. Translational arrest leading to SG formation typically occurs when the translation initiation factor eIF2α is phosphorylated at Ser51, which reduces the availability of the eIF2-GTP-$tRNA_i^{Met}$ ternary complex that is required for initiation (Kedersha et al., 1999). Several "sensor kinases" that phosphorylate eIF2α in response to various stresses have been identified, such as protein kinase R (PKR), PKR-like endoplasmic reticulum kinase (PERK), and heme-regulated

initiation factor 2α kinase (HRI) (Harding et al., 2000; McEwen et al., 2005; Srivastava et al., 1998). SG formation can also be induced when initiation is blocked in other ways, such as by pharmacological intervention using antibiotics, or by targeted knock-down of other specific translation initiation factors (Mazroui et al., 2006; Mokas et al., 2009).

Following the release of the 48S mRNP substrate for SG assembly, many other proteins are recruited which promote SG nucleation and growth. These additional "assembly-factors" are able to bind mRNAs and often are able to self-aggregate by virtue of their QN-rich prion-like domains, or by other protein-protein interactions (Anderson and Kedersha, 2008). Examples of SG proteins with these properties include TIA-1, TIAR, and G3BP (Gilks et al., 2004; Tourrière et al., 2001).

It is important to note however, that SGs are not simply static repositories of mRNA and protein that form during stress. They form rapidly (within 5-10 minutes of the onset of stress), and disassemble equally fast during recovery from stress (Kedersha et al., 2000). Following SG formation, many of the mRNAs and proteins within them are rapidly shuttled to other cell compartments. mRNAs in SGs are in dynamic equilibrium with translating polysomes, as well as with other cytoplasmic RNA granules called processing bodies (PBs), which likely function in mRNA decapping and degradation, and RNA-induced silencing (Buchan and Parker, 2009). For this reason SGs are thought to be sites of "RNA triage", where untranslated messages are sorted to various cellular fates during stress, such as re-entry into the translating pool, decapping and degradation in PBs, or perhaps long-term storage in other mRNPs. However, this hypothesis has yet to be proven, for several reasons. SGs have to date only been studied microscopically, and further elucidation of their functions awaits their biochemical purification and

reconstitution *in vitro*. Furthermore, all of the protein components found in SGs to date serve functions in other cell processes, and are only recruited there during stress. Therefore it has been difficult to assign any phenotypes observed when these components are disrupted to a specific role of SGs, and not to their functions elsewhere.

Chloroplast stress granules and the large Rubisco subunit

It was recently discovered that mRNP aggregates also form during stress in the chloroplast of the unicellular green alga, *Chlamydomonas reinhardtii* (Uniacke and Zerges, 2008). These aggregates were called chloroplast stress granules (cpSGs) because they share many similarities with the SGs found in the cytoplasm of mammalian cells and other eukaryotes. For example cpSGs form during high-light exposure, a condition that causes oxidative stress in photosynthetic organisms (Nishiyama et al., 2001), as well as during UV irradiation and nutrient deprivation. They also contain mRNAs released from polysomes, the small but not the large chloroplast ribosomal subunit, and the chloroplast homologue of PABP-1 (cPABP). Like SGs, cpSGs form rapidly following the onset of stress, they disassemble equally fast during recovery, and the mRNAs within cpSGs are in dynamic equilibrium with chloroplast polysomes. The discovery of cpSGs in an organelle of bacterial ancestry suggests that the formation of stress-induced RNA granules is a conserved feature across evolution, and that their functions may be particularly important for survival during stress.

Two key features distinguish cpSGs from SGs. First, they do not form in the cytoplasm, but in the chloroplast stroma. The mRNAs that localize to cpSGs are transcribed from the chloroplast genome, and are translated by the bacterial-like 70S

ribosomes of the chloroplast. It is the 30S subunit of the chloroplast ribosome that is recruited to cpSGs. Another feature that distinguishes cpSGs from SGs is the recruitment of a protein involved in photosynthesis, the large subunit of ribulose-1,5-bisphosphate carboxylase/oxygenase (Rubisco). Rubisco is the enzyme that is responsible for carbon assimilation into ribulose-1,5-bisphosphate in chloroplasts during the Calvin-Benson cycle, and for the oxygenation of ribulose bisphosphate during photorespiration (Spreitzer and Salvucci, 2002). This soluble enzyme is located in the proteinaceous stroma of the chloroplast, and comprises some 40-50% of the total protein in photosynthetic tissue; as such, it is likely the most abundant protein on Earth (Ellis, 1979). The Rubisco holoenzyme is a multi-subunit protein complex that is composed of eight copies of a large subunit (RBCL), and eight copies of a small subunit (RBCS). RBCS is encoded for by a gene family located in the nucleus, while RBCL is encoded for by a single gene in the chloroplast genome (Miziorko and Lorimer, 1983). The finding that RBCL alone is recruited to cpSGs suggests that whatever function it has in that compartment, it is independent of its role in photosynthesis.

Previous studies have shown that during oxidative stress, RBCL displays several characteristics that are consistent with a potential role as a cpSG assembly factor. *In vitro* biochemical analyses have shown that under oxidizing conditions RBCL is able to bind to RNA in a sequence-independent manner (Yosef et al., 2004). The RNA binding activity of RBCL was predicted at the N-terminal region of the protein because it has structural similarity to an RNA-recognition motif (RRM) found in certain RNA-binding proteins. The RRM and RNA binding activity of RBCL is conserved throughout a broad range of photosynthetic organisms (Cohen et al., 2006). Furthermore, the Rubisco

holoenzyme has been shown to disassemble during *in vivo* oxidative stress and *in vitro* oxidizing conditions, which result in the degradation of the RBCS subunit and the formation of high-molecular weight aggregates of RBCL (Knopf and Shapira, 2005). During oxidative stress, Rubisco has also been observed to localize to an insoluble fraction of cell lysates (Marín-Navarro and Moreno, 2006; Mehta et al., 1992). Finally, these characteristics of RBCL that are observed during stress or oxidizing conditions (holoenzyme disassembly, RNA binding activity, aggregation) are thought to be regulated by the reversible oxidation of specific cysteine residues (Cohen et al., 2005; Marín-Navarro and Moreno, 2006; Moreno et al., 2008). Therefore, RBCL shares several characteristics with SG assembly factors in that it can bind non-specifically to mRNA and aggregate during oxidative stress.

The majority of Rubisco in most algae and hornworts is localized to a spherical body within the chloroplast called the pyrenoid, as part of a carbon-concentrating mechanism (McKay and Gibbs, 1991). This region around the pyrenoid may also have some function in translation by the ribosomes of the chloroplast genetic system (Schottkowski et al., 2012; Uniacke and Zerges, 2007, 2009). Because cpSGs were discovered at the inner periphery of the pyrenoid, a model was proposed in which the disassembly of Rubisco during oxidative stress releases RBCL that is able to meet the mRNAs released from polysomes for the formation of cpSGs (Uniacke and Zerges, 2008).

Rubisco is one of the most extensively studied proteins, yet to date it has almost exclusively been studied in the context of its role in photosynthesis. The RNA binding activity and cpSG recruitment of RBCL are recent discoveries, and the biological

significance of these observations has yet to be elucidated. Interestingly, there several other examples of metabolic enzymes that are able to "moonlight" as RNA binding proteins (Cieśla, 2006). Several enzymes involved in glycolysis, such as enolase, glyceraldehyde-3-phosphate dehydrogenase, and lactate dehydrogenase are able to bind RNA (Hernández-Pérez et al., 2011; Nagy and Rigby, 1995; Pioli et al., 2002). Aconitase and NAD(+)-dependant isocitrate dehydrogenase participate in the TCA cycle, and both are able to bind RNA (Elzinga et al., 1993; Klausner and Rouault, 1993). It is generally thought that the dual function RNA binding activity of these enzymes allows for the regulation of gene expression in the metabolic pathways in which they participate (Cieśla, 2006).

Goal of thesis and contribution of colleagues

This project was initiated when another graduate student in our lab investigated the possibility that cpSGs are involved in oxidative stress tolerance. It was found that under the oxidizing conditions which induce Rubisco disassembly and RBCL recruitment to cpSGs, a *Chlamydomonas* mutant that lacks the large subunit of Rubisco is impaired in oxidative stress tolerance, while a mutant that lacks the small Rubisco subunit is hypertolerant to oxidative stress (Yu Zhan, unpublished data). The goals of my work here were first to confirm that RBCL is required for oxidative stress tolerance in *Chlamydomonas*; second, to explore the potential protective mechanisms by which RBCL is able to confer oxidative stress tolerance; third, to characterize the biochemical properties of RBCL that may explain its requirement for oxidative stress tolerance; and finally, to explore whether the protective properties of RBCL reflect a function of cpSGs.

Because RBCL is also required for Rubisco function in the Calvin-Benson cycle, my analyses were controlled by comparative examination of the RBCS-deficient strain, which also lacks Rubisco function. To achieve the first goal, the assembly state of RBCL in the hypertolerant RBCS-deficient strain was genetically manipulated, and the effects of this manipulation on the resulting strains' oxidative stress tolerance were observed. To achieve the second goal, I attempted to measure the relative amounts of oxidative damage to the proteins and lipids of wild type, RBCL-deficient, and RBCS-deficient strains of *Chlamydomonas*, in order to determine whether the mitigation of oxidative damage to these cellular components is the mechanism by which RBCL is able to provide oxidative stress tolerance. To achieve the third and fourth goals, I developed a novel technique for the biochemical subfractionation of *Chlamydomonas* cell lysates that allowed me to identify a previously uncharacterized subpool of RBCL that functions in oxidative stress tolerance. In addition, I also describe several exploratory experiments and unsuccessful approaches, which are documented in the appendix.

The unicellular green alga *Chlamydomonas reinhardtii* was used here to study the stress function of RBCL. *Chlamydomonas* has a long history as a model organism for studying numerous biological processes, such as photosynthesis, cell motility, cell cycle, light recognition, and chloroplasts biogenesis. It grows vegetatively as haploid cells, and numerous mutants are available from a stock center. Mating can be induced by manipulating nutrient concentrations, allowing for genetic crosses and tetrad analysis. In addition, there are well established techniques for the transformation of its nuclear and chloroplast genomes. Important for this study is the ability of *C. reinhardtii* to grow

heterotrophically when provided with a reduced carbon source, meaning that mutants of photosynthesis are completely viable.

The work described in this thesis was part of a collaborative project with Yu Zhan, a PhD student under the supervision of Dr. Zerges. Yu Zhan and I contributed equally to the manuscript, and her work described throughout this thesis.

Chapter 2: Materials and Methods

Manipulation of *Chlamydomonas*

The *Chlamydomonas reinhardtii* strains used here were wild-type, *4A+* (CC-4051), 1B$^-$, CC620, CC621(*Chlamydomonas* Stock Center); *ΔrbcL-MX3312*, *MX3312* (Dr. Genhai Zhu, Pioneer Hi-Bred) (Satagopan and Spreitzer, 2004); *ΔrbcS-dim1*, CAL005.01.13 (Dent et al., 2005), 12D$^-$ (this study); Δ*rbcL;*Δ*rbcS* (this study); and Δ*rbcS-RBCS2*, (this study). Both nuclear genes encoding RBCS in *ΔrbcS-dim1* are disrupted. Strains *ΔrbcL-MX3312, ΔrbcS-dim1,* Δ*rbcL;*Δ*rbcS*, are non-photosynthetic, but fully viable under heterotrophic conditions, with acetate provided as an exogenous energy source (Satagopan and Spreitzer, 2004). Unless otherwise indicated, cell cultures were grown to mid-logarithmic phase (2-4 x 10^6 cells/ml) in a 24^{o}C orbital shaker, in Tris-Acetate Phosphate (TAP) media (Harris, 1989). Strains 4A$^+$, *ΔrbcL-MX3312*, *ΔrbcS-dim1*, Δ*rbcL;*Δ*rbcS*, Δ*rbcS-RBCS2* were used for either stress tolerance assays, biochemical analyses, or both. Strains CC620 and CC621 were used for mating to generate gamete autolysin for nuclear transformations (Harris, 1989). Strains 1B$^-$, 12D$^-$, *ΔrbcL-MX3312*, and *ΔrbcS-dim1* were used for genetic crosses to generate the Δ*rbcL;*Δ*rbcS* double mutant (Harris, 1989). *ΔrbcS-dim1* was used for chloroplast transformation and for nuclear transformation to generate Δ*rbcL;*Δ*rbcS* and Δ*rbcS-RBCS2* strains, respectively. Due to their deficiencies in the photosynthetic electron transport chain, the *ΔrbcL-MX3312*, *ΔrbcS-dim1*, Δ*rbcL;*Δ*rbcS* mutants produce ROS upon illumination and are light-sensitive. Therefore, for all stress assays and biochemical analyses, the cultures were grown and tested under in the dark.

Generation of mutants

The Δ*rbcS-RBCS2* rescue mutant was obtained by transforming *ΔrbcS-dim1* with the *RBCS2* gene from plasmid pSS2 (Khrebtukova and Spreitzer, 1996) by glass bead agitation (Kindle, 1990). Prior to nuclear transformation, *ΔrbcS-dim1* was treated with gamete autolysin to partially degrade the cell wall. Autolysin is produced and secreted by *Chlamydomonas* gametes during mating. To obtain autolysin, strains CC620 and CC621 were crossed in liquid TAP-N media (Harris, 1989). The gametes from this culture were pelleted by centrifugation for 5 minutes at 5,000 x g, and the resulting supernatant, which contained the cell wall-degrading autolysin enzyme, was collected. 300 ml of *ΔrbcS-dim1* culture was grown to 1-2 x 10^6cells/ml, pelleted as described above, and resuspended in the autolysin-containing supernatant for cell wall degradation. After 30 minutes, the *ΔrbcS-dim1* cells were resuspended in 2.5 ml of selective media, and transformed by vortexing 300 µl of cells in glass test-tubes, in the presence of 300 mg of glass beads, 100 µl 20% PEG 6000 and 100 ng of an EcoRI-HindIII linear fragment from plasmid pSS2 that contains *RBCS2*. Δ*rbcS-RBCS2* transformants were selected on "high salt minimal" (HSM) medium for photoautotrophic growth and confirmed by PCR using primers 5'-TCATTGCCAAGTCCTCCGTCTC-3'and 5'- GGAAATGGGAGGGAGAAGAGGT-3'. These primers anneal to the coding sequence of both *RBCS* genes; in *RBCS1* they amplify an 877 base pair product, and in *RBCS2* they amplify a 1019 base pair product. DNA was isolated for PCR analysis as described previously (Murray and Thompson, 1980).

A Δ*rbcL;*Δ*rbcS* double mutant was obtained by disrupting the *rbcL* gene by homologous recombination in the *ΔrbcS-dim1* strain. This was achieved using chloroplast transformation, as described previously (Johnson et al., 2010) by particle bombardment

(Boynton and Gillham, 1993). Cells were grown to mid-logarithmic phase (2-4 x 10^6 cells/ml), then 300 µl containing 3 x 10^6 cells were plated on agar-solidified TAP media and allowed to grow for 3-5 days to form a dense, confluent layer. Approximately 5 mg of gold particles coated with 5 µg of plasmid ΔrbcL-2 (containing the spectinomycin-resistance gene *aadA*) was used for bombardment per transformation plate (Johnson et al., 2010). Transformants were selected on solid media containing 100 µg/ml spectinomycin. To ensure chloroplast genome homoplasmicity, transformants were propagated for several generations in liquid media containing 150 µg/ml spectinomycin, followed by single colony isolation on solid media containing 500 µg/ml spectinomycin.

Alternatively, genetic crosses were used to generate a Δ*rbcL;*Δ*rbcS* double mutant (Harris, 1989). Δ*rbcL*-MX3312 and Δ*rbcS-dim1* are of the same mating type (mt+) and therefore, cannot be crossed. The *rbcL* gene is encoded by the chloroplast genome, which is uniparentally inherited from the mt+ parent, while the *RBCS* locus is in the nuclear genome and is transmitted by Mendelian-inheritance. Therefore, I needed to generate an mt- strain carrying the deleted *RBCS* locus of Δ*rbcS-dim1*. To do this, Δ*rbcS-dim1* was crossed to a wild-type mt- strain ($1B^-$), to generate a Δ*rbcS* mt- strain. The resulting progeny were screened for the dual phenotypes of obligate heterotrophic growth (indicating RBCS-deficiency) and the ability to mate with an mt+ strain. One of these progeny ($12D^-$) fulfilled these criteria and was crossed to *ΔrbcL-MX3312* to generate Δ*rbcL;*Δ*rbcS* progeny.

Δ*rbcL;*Δ*rbcS* double mutants were verified by PCR analysis to confirm the absence of *rbcL* and both *RBCS* genes. Primers 5'-GCTCGAGGTGCTGCAGCTAACC-3' (forward) and 5'-ACGTGCGACCCGATGTGGTAC-3' (reverse) were used to confirm

the absence of *rbcL*. The forward primer anneals to the *rbcL* coding sequence, while the reverse primer anneals to a region in the 3'-UTR of the gene that remains following transformation. Therefore, the absence of a PCR product indicates the absence of the *rbcL* gene. The *RBCS* primers described above were used to confirm the absence of *RBCS1* and *RBCS2* in double mutants. In this case, the absence of the 877 bp and 1019 bp PCR products indicates the absence of *RBCS1* and *RBCS2*.

Determination of oxidative stress tolerance

Δ*rbcL;*Δ*rbcS* and Δ*rbcS-RBCS2* were tested for their ability to survive and remain viable during oxidative stress. Cultures of each strain were exposed to exogenously added 4mM H_2O_2, and cell survival and viability were monitored at one hour intervals for eight hours. Survival was determined as the percentage of cells that exclude Trypan Blue, a dye that is selective for dead cells (Strober, 2001). Viability was determined as the percentage of cells that are able to divide and form colonies on non-selective agar-solidified TAP media. Each test was performed for both strains a minimum of six times, and significance was determined using two sample t-tests ($p \leq 0.05$).

H_2O_2 quantification in media

Quantification of H_2O_2 in liquid media was performed as described previously (Shao et al., 2008). At each time point, 500 µL of culture was centrifuged at 17,000 x g for 5 minutes, and the supernatants were added to an equal volume of 1M KI. Following 15 minutes of incubation at room temperature, the formation of iodine was determined by

measuring OD at 390 nm. The obtained values were compared to a standard curve prepared from known concentrations of H_2O_2.

Molecular damage analyses

Oxidative damage to proteins and lipids were examined following the exposure of wild-type, *ΔrbcL-MX3312* and *ΔrbcS-dim1* to various challenges: 4mM H_2O_2, 6 μM rose bengal under 100 $\mu E \cdot m^{-1} \cdot s^{-2}$ light intensity, 1 μM methyl viologen under 100 $\mu E \cdot m^{-1} \cdot s^{-2}$ light intensity, 1 μM cadmium (Cd^{2+}), 1 μM copper (Cu^{2+}), 40°C, 2,000 $\mu E \cdot m^{-1} \cdot s^{-2}$ light intensity, and 1, 200 mJ UV irradiation. All stress exposures were for 15 minutes, with the following exceptions: UV irradiation, which was delivered using the Stratalinker (*Agilent Technologies* Inc); H_2O_2-stress, which was over a 1 hr time course with samples taken at 15, 30, and 60 min.

Protein oxidation was analyzed by detecting the presence of carbonyl groups in total protein extracts using the OxyBlot protein oxidation detection kit (Millipore). Following the indicated stresses, 15 ml of cell culture was centrifuged at 3,000 x g for 5 minutes and the resulting cell pellets were broken by beat-beating in 75 μl of protein extraction buffer (50 mM Tris-Cl ph 8.0, 1 mM EDTA, 50 μM NaCl, 1 mM PMSF, 100 mM DTT). Samples of 20 μg of protein obtained from cell pellets were derivatized to 2,4-dinitrophenylhydrazone, and analyzed as described by the manufacturer's instructions, by 12% SDS-PAGE and Western blotting. Samples were loaded based on the amount of total protein as determined by the Bradford Assay (Sigma), and controlled by loading of a ribosomal protein (S-20). The amount of protein carbonylation in H_2O_2-stressed cells was determined using imageJ, by quantification of ECL signals. The level of protein

carbonylation in *ΔrbcL-MX3312* prior to stress was used as an internal standard, and designated as 100%. This was done because the goal was to determine whether oxidative protein damage was significantly different in wild type or *ΔrbcS-dim1* relative to *ΔrbcL-MX3312*. Significance was determined by one sample t-tests using the 100% signal of *ΔrbcL* as the null hypothesis ($p \leq 0.05$).

Lipid Peroxidation was analyzed by detecting the presence of thiobarbituric acid reactive species using the Quantichrome TBARS Assay kit (BioAssay Systems). Cell pellets obtained as described above were pelleted and resuspended to 2.5 x 10^7 cells/ml in 1X ice-cold Phosphate-Buffered Saline, pH 7.4 (PBS), and disrupted by sonication at 30% intensity for one minute in 10 second on/off cycles. The resulting lysates were analyzed as described by the manufacturer's instructions. Sample values were standardized based on the amount of chlorophyll present, as described previously (Porra, 2002).

Green-native PAGE and heme staining

Cells from 50 ml of culture grown to mid-log phase were either treated with 4 mM H_2O_2 for 15 minutes or left untreated, then centrifuged at 5,000 x g for 5 minutes and resuspended in 500 µl ice cold MKT-buffer [25 mM $MgCl_2$, 20 mM KCl, 10 mM Tricine-Cl pH 7.5, 10% (w/v) protease inhibitor cocktail (Sigma-Aldrich)]. The cells were broken by sonication at 30% intensity for one minute in 10 second on/off cycles. Green-native PAGE was performed as described previously (Allen and Staehelin, 1991). Cell lysates equivalent to 20 µg of chlorophyll were centrifuged at 17,000 x g for 5 minutes at 4^{o}C and the pellets were resuspended in 40 µl of freshly prepared membrane

solubilization buffer (10 mg/ml detergent (0.45% β-dodecyl maltoside, 0.45% octyl glucoside, 0.1% lithium dodecyl sulphate), 50 mM Bis-Tris pH 7.0, 750 mM aminocaproic acid, 10% glycerol, ponceau salt), resulting in a detergent:chlorophyll ratio of 20:1. After a 30 minute incubation on ice with occasional mixing, the solubilized membranes were separated using an 8% polyacrylamide gel (100:1 acrylamide:bis-acrylamide) run at 15 mA for 2 hours at 4^{o}C. Following electrophoresis, the gel was stained for the peroxidase activity of heme-containing protein complexes as described previously (Thomas et al., 1976). The gel was immersed into a staining solution (70% of 250 mM Sodium Acetate, ph 5.0 and 30% of 6.3 mM 3,3',5,5'-tetramethylbenzidine dissolved in methanol) with gentle agitation for 2 hours. Heme-staining was revealed by the addition of 30 mM H_2O_2 for 30 minutes, and stabilized by transferring the gel to a solution containing 30% isopropyl alcohol and 70% 250 mM Sodium Acetate, pH 5.0.

Pulse labelling of proteins

1.2 x 10^7 cells grown in the dark to mid-log phase in TAP medium were either stressed by the addition of 4 mM H_2O_2 for 15 min or left untreated, followed by pelletting and resuspension in 300 µL of sulfate-depleted TAP. 10 µg/ml cycloheximide was added for 5 min in dim light followed by the addition of 50 µL ^{35}S as H_2SO_4 (100 µCi) for 20 min. Cells were washed once in 500 µL 50 mM Tris-Cl pH 7.4 followed by breakage in 80 µL protein extraction buffer by bead-beating. Pellet and supernatant fractions were separated by centrifugation at 17, 000 x g for 5 min and denatured in 100 µL of 1X SDS-loading buffer (Laemmli, 1970). 50 µL of each sample, equivalent to 6 x 10^6 cells, was fractionated on a 7.5-15% SDS-polyacrylamide gel containing 6M urea. The gel was then

stained with Coomassie Blue, dried, and the presence of radiolabelled protein was visualized with a phosphoimager (Trio imager, Typhoon Inc.).

Determination of RBCL amount in *ΔrbcS-dim1*

Approximately 6 x 10^6 cells from mid-log cultures of wild type, *ΔrbcL-MX3312*, and *ΔrbcS-dim1* were boiled in 1X SDS loading buffer (Laemmli, 1970). 10%, and 1% of the wild-type sample volume was spiked into 90% and 99% of *ΔrbcL-MX3312* sample volume for the wild type dilution series. 20 µl of each sample was separated by SDS-PAGE, transferred to nitrocellulose membranes, and RBCL was detected with rabbit polyclonal antiserum (1:30,000) (Agrisera AS03037) for 2 h at room temperature. Prior to the addition of αRBCL antisera, membranes were cut horizontally at approximately 30 kDa to avoid detection of cross reacting bands. Detection of a 30S ribosomal protein (S-20) was used as a loading control. Goat anti rabbit secondary antibody (1:10,000) (KPL) was used for 1 h at room temperature.

Cellular subfractionation

Analytical subcellular fractionation was performed as described previously, with some modifications (Schottkowski et al., 2012). Cells cultures of wild type and *ΔrbcS-dim1* were either treated with 4mM H_2O_2 for 30 minutes or left untreated, then pelleted and resuspended in 12 ml ice cold MKT-buffer. The cells were broken by three passes through a chilled French Pressure Cell, and breakage was verified by light microscopy (400× and 1,000× magnification). Cell lysates were centrifuged at 100,000 x g for 1 hour at 4^{o}C. The supernatant was removed and stored at -80^{o}C while the pellet was

resuspended in 2 ml MKT buffer containing 2.5 M sucrose. A 750 µl 2.2M sucrose cushion was added on top of the resuspension, followed by a 10 ml 0.5 M-2.0 M linear sucrose gradient. The gradient was centrifuged at 100,000 x g for 16 hours at 4^{o}C, and then collected in 750 µl fractions. The pellet of the gradient was resuspended in 750 µl MKT, and stored at -80^{o}C along with the gradient fractions. Equal proportions of each fraction were analyzed by SDS-PAGE and Western blotting. RBCL was detected with rabbit polyclonal antiserum (1:5,000) (provided by Dr. Spreitzer) for 2 hrs at room temperature. Goat anti rabbit secondary antibody (1:10,000) (KPL) was used for 1 h at room temperature.

Differential centrifugation

Cells from a 75 ml culture were pelleted by centrifugation at 5,000 x g for 5 minutes at room temperature and resuspended in 5-ml ice cold MKT-buffer. The cells were broken by three passes through a chilled French Pressure cell at 1,000 psi, and breakage was verified by light microscopy (400× and 1,000× magnification). The lysate was centrifuged at 3,200 x g for 1 minute to remove unbroken cells and the supernatant was then centrifuged again at 17,000 x g for 20 minutes at 4^{o}C. The resulting supernatant was removed and stored at -80^{o}C (fraction S17), while the pellet (fraction P17) was resuspended in the same volume of MKT-buffer with 2% Triton X-100 and incubated on a rocker for 15 minutes at room temp. Fraction P17 was then centrifuged again at 17,000 x g for 20 minutes, to generate supernatant (fraction P17-TS) and pellet (fraction P17-TI) fractions. P17-TS was removed and stored at -80^{o}C, and fraction P17-TI was resuspended in MKT-buffer and stored at -80^{o}C. Prior to freezing, aliquots of each fraction were

removed and prepared for SDS-PAGE and immunoblot analysis. RBCL was detected with a rabbit polyclonal antiserum (1:30,000) (Agrisera AS03037) for 2 h at room temperature. Prior to the addition of αRBCL antisera, membranes were cut horizontally at approximately 30 kDa to avoid detection of cross reacting bands. Goat anti rabbit secondary antibody (1:10,000) (KPL) was used for 1 h at room temperature. Replicate gels were stained using the ProteoSilver Silver Stain kit (Sigma), according to the manufacturer's instructions.

Chapter 3: Results

RBCL has a dual function in controlling oxidative stress tolerance in *Chlamydomonas*

It was previously demonstrated that a Rubisco mutant that is RBCL deficient, called here *ΔrbcL-MX3312*, is significantly impaired in oxidative stress tolerance. When challenged with exogenously added 4 mM H_2O_2, cultures of *ΔrbcL-MX3312* died more rapidly over an 8 h time course than those of wild type, in an assay for cell survival (Yu Zhan, unpublished data). Conversely, an RBCS deficient mutant, called here *ΔrbcS-dim1* had *enhanced* survival as compared to wild type (Yu Zhan, unpublished data). The hypertolerance of *ΔrbcS-dim1* was even observed under a more stringent assay, where the ability to remain viable and form colonies was measured (Yu Zhan, unpublished data). The differences in survival and viability between these strains were not due to unequal rates of H_2O_2 breakdown in the media (Fig. 1). *ΔrbcL-MX3312* and *ΔrbcS-dim1*differ only in which subunit of Rubisco is absent, yet displayed opposing stress tolerance phenotypes. This appeared to suggest that RBCL is *required* for oxidative stress tolerance, but when present in the absence of its Rubisco assembly partner, is able to confer *enhanced* oxidative stress tolerance. However, several alternate possibilities could not be discounted that might explain these opposing phenotypes. For example, the hypertolerance phenotype of *ΔrbcS-*

dim1 could be due to background genetic effects, such as modifier mutations of genes involved in H_2O_2 degradation or other antioxidant capabilities, which enhance its survival during stress. Alternatively, there may exist an unknown alternate function of RBCS,

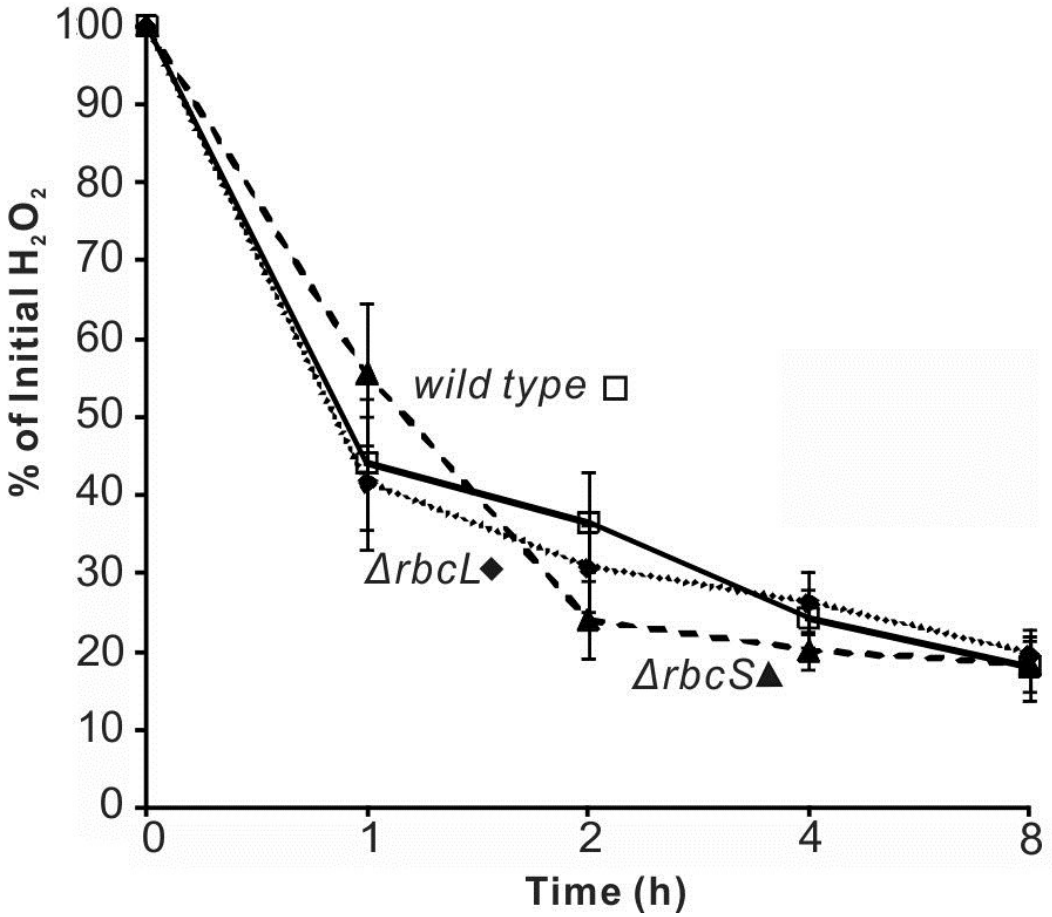

Figure 1) The *ΔrbcL* and *ΔrbcS* mutants showed wild-type levels H_2O_2 breakdown in the media. H_2O_2 concentration in the medium of wild type, *ΔrbcL-MX3312* and *ΔrbcS-dim1* strains was measured at the indicated time points, and graphed as the percentage of the initial concentration (4 mM). Error bars indicate 1 standard error.

perhaps in signalling cell death during stress. This function would be lost in *ΔrbcS-dim1* and perhaps enhanced when RBCS is present in the absence of its Rubisco assembly partner, resulting in the impaired survival of *ΔrbcL-MX3312*. There is precedence for an organellar metabolic protein having a dual function in signalling programmed cell death: Cytochrome c, when released from mitochondria into the cytosol, initiates an apoptotic program (Liu et al., 1996). A similar role for RBCS was considered here because it was previously observed *in situ* that RBCS accumulates outside of the chloroplast under certain stress conditions (Uniacke and Zerges, 2008).

In order to test these alternative hypotheses, I took a genetic approach. If the high-tolerance phenotype of *ΔrbcS-dim1* is due to background genetic effects, then rescuing the mutant with a gene encoding RBCS should have no effect on its stress tolerance. Therefore, I transformed the *ΔrbcS-dim1* nuclear genome with a wild-type copy of *RBCS2* (Khrebtukova and Spreitzer, 1996). Rescued mutants were expected to form a functional Rubisco holoenzyme and, therefore, were selected for their ability to grow photoautotrophically. A photosynthetic colony recovered following transformation was tested by PCR for the presence of the introduced *RBCS2* gene (Supplementary Fig. 1a). The primers used in this assay anneal to both *RBCS1* and *RBCS2*, amplifying 877 base pair and 1019 base pair products from each gene, respectively. In the transformant, the expected 1 kb *RBCS2* PCR product was observed. For unknown reasons, in this experiment only the *RBCS1* PCR product was amplified in the control strain, *ΔrbcL-MX3312*. Both genes are present in *ΔrbcL-MX3312* however, as seen in Supplementary Fig. 1e. As expected, neither PCR product was observed in *ΔrbcS-dim1*. The transformed colony was also able to grow in the presence of the antibiotic bleomycin, for which

resistance was provided by the *ble* gene when the *RBCS* gene family was initially knocked out (Dent et al., 2005). The rescued mutant was called Δ*rbcS-RBCS2*, and its H_2O_2-tolerance was tested as described above (Fig. 2a and b). Survival was determined by the percentage of live cells at each time point, on the basis of their non-staining with the dye Trypan blue (Strober, 2001). Viability was determined as the percentage of the initial cells that are able to grow and form colonies at each time point. I observed that Δ*rbcS-RBCS2* had reduced survival and viability in response to H_2O_2 relative to its parental strain, down to the level of the wild-type strain. Therefore, the hypertolerance phenotype of *ΔrbcS-dim1* is not due to background genetic effects.

Next I asked if the high-tolerance *ΔrbcS-dim1* phenotype *is* in fact RBCL-dependent. If this is the case, then a double mutant lacking both RBCS and RBCL is expected to be impaired in stress tolerance, to the same extent that *ΔrbcL-MX3312* is. To test this, I created a double mutant by knocking out the *rbcL* gene from the chloroplast genome of *ΔrbcS-dim1*, using particle bombardment with an *rbcL* deletion cassette (Johnson et al., 2010). Because the chloroplast genome is present in c.a. 100 copies in *Chlamydomonas* (Higgs, 2009), selection was required for several generations to ensure that all copies were transformed (see Materials and Methods). Homoplasmic transformants were identified using diagnostic PCR, in which the forward primer annealed to the *rbcL* coding sequence, and the reverse primer annealed to the 3'-UTR of the gene, generating a band of 829 bp. Thus, a PCR product indicated the presence of untransformed copies of the chloroplast genome, whereas no PCR product indicated homoplasmic clones with the *rbcL*-deletion (Supplementary Fig. 1b). As seen in the first and second lanes, respectively, *rbcL* could not be detected in *ΔrbcL-MX3312,* but could

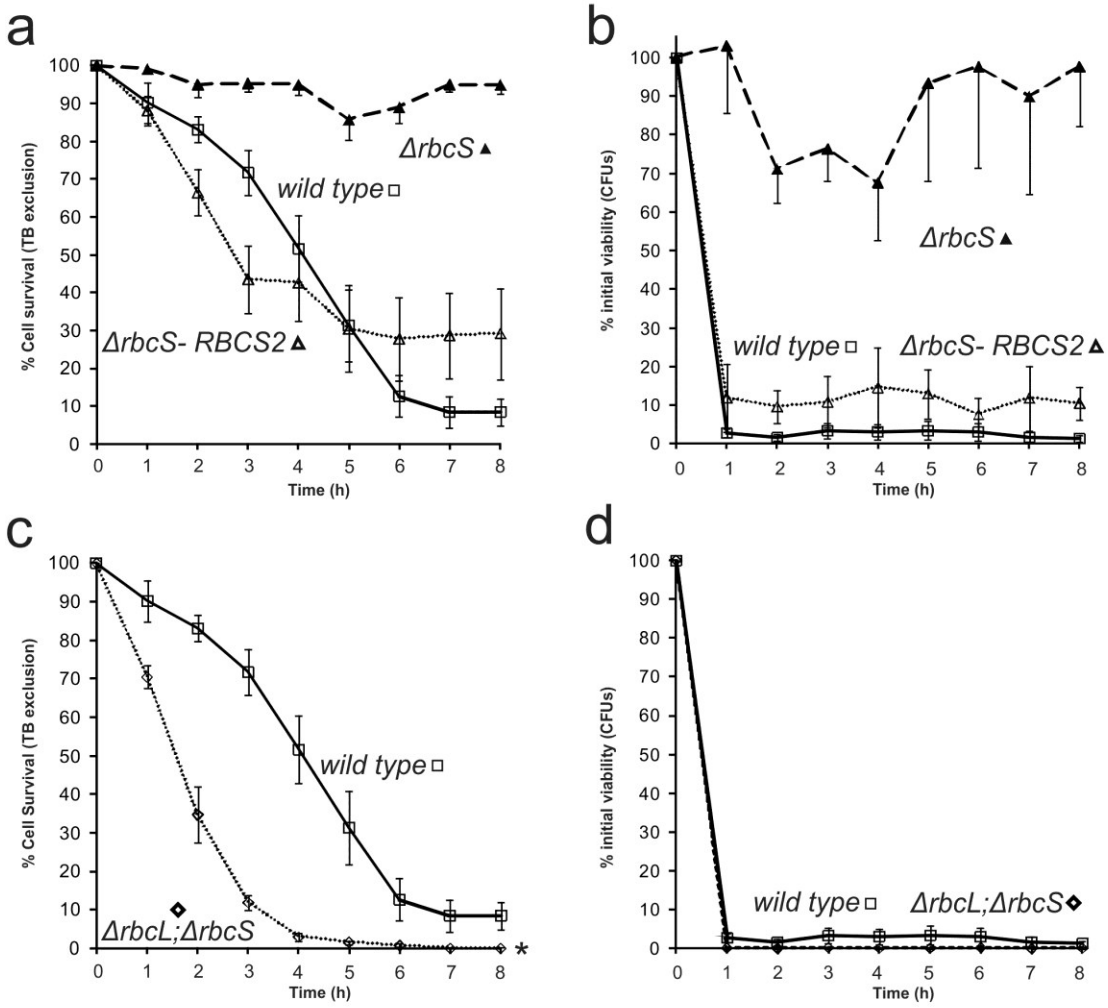

Figure 2) Time course assays of cell survival and viability reveal that RBCL is the major determinant of H_2O_2 tolerance. The mean percentage of initial survival as measured by Trypan Blue exclusion **(**a, c, e), and the mean percentage of initial viability as measured by CFU concentration (b, d, f), in response to 4 mM H_2O_2. a) and b) show the H_2O_2 tolerance of *ΔrbcS-RBCS2*relative to wild type and *ΔrbcS-dim1.* c) and d) show the H_2O_2 tolerance of the stable *ΔrbcL;ΔrbcS* double mutant obtained by mating. Error bars indicate one standard error.

be detected in the parental strain used for transformation, *ΔrbcS-dim1*. Lanes 3-6 show several transformants that lacked *rbcL* following several generations of growth without selection. Following the identification of transformants, one was tested for its ability to survive and remain viable after exposure to 4 mM H_2O_2, as described above. I observed that this double mutant had reduced survival and viability in response to H_2O_2, relative to *ΔrbcS-dim1* (Supplementary Fig. 2a and b). However these phenotypes were not as severe as those of *ΔrbcL-MX3312*, as would be expected if RBCL were the sole determinant of the elevated tolerance phenotype of *ΔrbcS-dim1*. For this reason, I suspected that the double mutant strain obtained by transformation may not have been homoplasmic, had retained some *rbcL* expression, and was in the process of reverting to the parental genotype. Upon further PCR analysis after several more generations without selection, it was confirmed that all of the Δ*rbcL;*Δ*rbcS* double mutants obtained by chloroplast transformation had indeed reverted to the *ΔrbcS-dim1* genotype, and the *rbcL* gene could be detected in them (Supplementary Fig. 1c).

As a second approach to create a Δ*rbcL;*Δ*rbcS* strain, I crossed *ΔrbcS-dim1*to *ΔrbcL-MX3312*. In *Chlamydomonas* genetic crosses, the nuclear genome is inherited in a Mendelian pattern, while the chloroplast genome is inherited uniparentally (Harris, 1989). The parent that transfers its chloroplast genome to the progeny is called mating-type + (mt+), the parent that does not transfer its chloroplast genome is called mating-type – (mt-), and the locus that determines mating type is located in the nucleus. Both *ΔrbcS-dim1* and *ΔrbcL-MX3312* are mt+, therefore *ΔrbcS-dim1* was first crossed to a wild-type mt- strain, where 50% of the *RBCS*-null progeny were compatible for mating with *ΔrbcL-MX3312*. One of these Δ*rbcS* mt- progeny was then crossed with *ΔrbcL-*

MX3312. Because *ΔrbcL-MX3312* is mt+, all progeny are expected inherit its *rbcL*-deficient chloroplast genome. 50% of the progeny from this cross are expected to be wild-type for *RBCS*, while 50% are expected to be *RBCS*-deficient. Therefore, in order to identify Δ*rbcL;*Δ*rbcS* mutants, it was sufficient to use PCR to screen for progeny that lack the *RBCS* genes. Several mutants were identified that had no *RBCS* PCR products (Supplementary Fig. 1e). The progeny were also tested for the presence of the *rbcL* gene, which was undetected in them (Supplementary Fig. 1d). As an added assurance, the progeny that lacked both *rbcL* and the *RBCS1,2* locus were also found to be resistant to both spectinomycin and bleomycin, since resistance cassettes to these two antibiotics were used for knocking out *rbcL* and *RBCS* in the parental strains, respectively (Dent et al., 2005; Satagopan and Spreitzer, 2004). Once an Δ*rbcL;*Δ*rbcS* double mutant was identified, its tolerance to H_2O_2 was examined as before (Fig. 2c and d). I found that this double mutant had greatly reduced survival and viability after exposure to H_2O_2, to the same level as *ΔrbcL-MX3312*. This result shows that the high tolerance phenotype of *ΔrbcS-dim1* requires a dual function of RBCL, one that is independent of the enzymatic activities of Rubisco.

RBCL in *ΔrbcS-dim1* is greatly reduced relative to wild type

The finding that RBCL is required for oxidative stress tolerance independently of its role in photosynthesis and photorespiration suggests that there is an alternate pool of the protein that is dedicated to this dual function. In the absence of Rubisco, this pool likely exists as the major form of RBCL in *ΔrbcS-dim1*. It was previously shown that in the absence of their assembly partners, the expression of subunits in photosynthetic

protein complexes is greatly reduced (Choquet et al., 2003; Minai et al., 2006; Wostrikoff et al., 2004). Indeed, another *RBCS* deletion mutant used in a previous study had reduced level of RBCL expression (Khrebtukova and Spreitzer, 1996). Therefore it is expected that *ΔrbcS-dim1* retains only a fraction of the wild-type level of RBCL. To examine this, I compared the amount of RBCL in *ΔrbcS-dim1* to that in wild type (Fig. 3). Total cell lysates from wild type, *ΔrbcS-dim1* and *ΔrbcL-MX3312* were separated by SDS-PAGE and analyzed by Western blotting. As expected, RBCL was undetected in *ΔrbcL-MX3312*. Comparison to a dilution series of wild-type lysate revealed that *ΔrbcS-dim1* contains c.a. 1-2% of the wild-type RBCL amount. Although this result confirms that RBCL expression in *ΔrbcS-dim1* is reduced, it nonetheless must be responsible for this strain's hypertolerance to H_2O_2. Because wild type also displayed RBCL-dependent tolerance to H_2O_2, the dual function pool of RBCL likely exists amongst the background of the Rubisco pool.

A minor pool of RBCL localizes to chloroplast translation membranes in wild type

It seemed likely that a secondary pool of RBCL, with the dual function of promoting oxidative stress tolerance, would have altered biochemical properties. Previous reports have shown that under the oxidizing conditions associated with H_2O_2-induced stress, Rubisco forms high-molecular weight aggregates, or localizes to a membrane fraction of the cell, or both (Marín-Navarro and Moreno, 2006; Mehta et al., 1992). To explore whether a potential membrane localization of RBCL is involved in its dual function, I employed a recently developed technique for the analytical subcellular localization of membrane proteins, where membranes obtained from cell lysates are

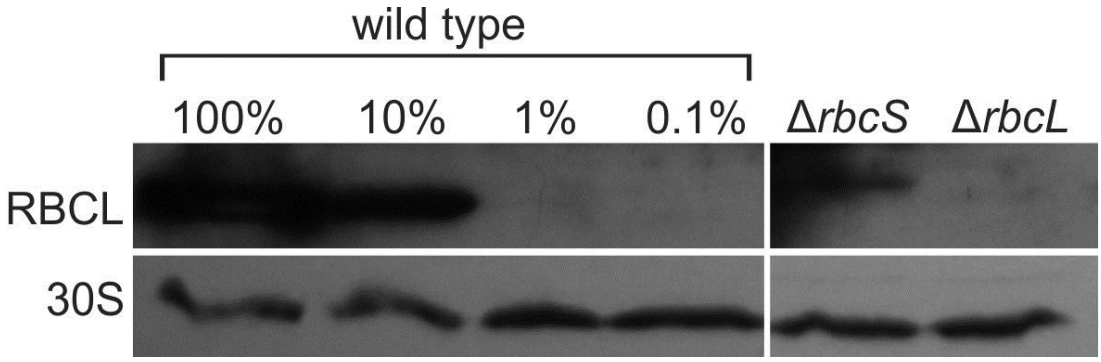

Figure 3) The *ΔrbcS* mutant has a reduced amount of RBCL relative to wild type. The amount of RBCL in the wild-type, *ΔrbcS-dim1* and *ΔrbcL-MX3312* mutant strains was analyzed by SDS-PAGE and immunoblot analyses. Dilutions of the wild-type cell lysate were supplemented with lysate from the *ΔrbcL-MX3312* strain to maintain a constant amount of total protein in each lane. An r-protein of the 30S subunit of the chloroplast ribosome was used as a loading control.

separated in a sucrose gradient based on their buoyancy (Schottkowski et al., 2012). Membranes were isolated from wild type and *ΔrbcS-dim1* cell lysates both prior to and following exposure of cell cultures to 4 mM H_2O_2, after which the localization of RBCL within them was examined (Fig. 4a and b). Following cell breakage, the lysates were ultracentrifuged to separate supernatant (S) and pellet fractions. The pellets were then separated by ultracentrifugation in a 0.5 M-2.0 M sucrose gradient, during which membranes within them are expected to migrate to their buoyant density in the gradient. Non-membranous material in the pellets was expected to either not float into the gradient, or to pellet again if sufficiently dense. Fractions from each gradient were collected and analyzed by Western blotting in equal volumes, in order to represent their original proportions in the cell. The results of the experiment that are shown here are preliminary, and are included for the purpose of documentation.

It was previously shown that in this experiment, soluble cell markers (i.e. for the chloroplast stroma and the cytosol) such as free ribosomal subunits and HSP70 remain in the supernatant, while thylakoid membranes float out from the pellet and localize to fractions 7-10 (Schottkowski et al., 2012). The denser fractions below the thylakoids contain chloroplast membranes that specialize in the biogenesis of photosynthetic complexes, and ribosomes and other translation factors localize there (fractions 12-14).

The results of my experiment showed that in wild type prior to stress, a minor amount of RBCL floated in the sucrose gradient, indicating its localization to membranes (lanes 9-14 in Fig. 4a). Rubisco is a soluble protein complex located in the chloroplast stroma, and as expected, most RBCL localized to the supernatant fraction (S) (Fig. 4b,

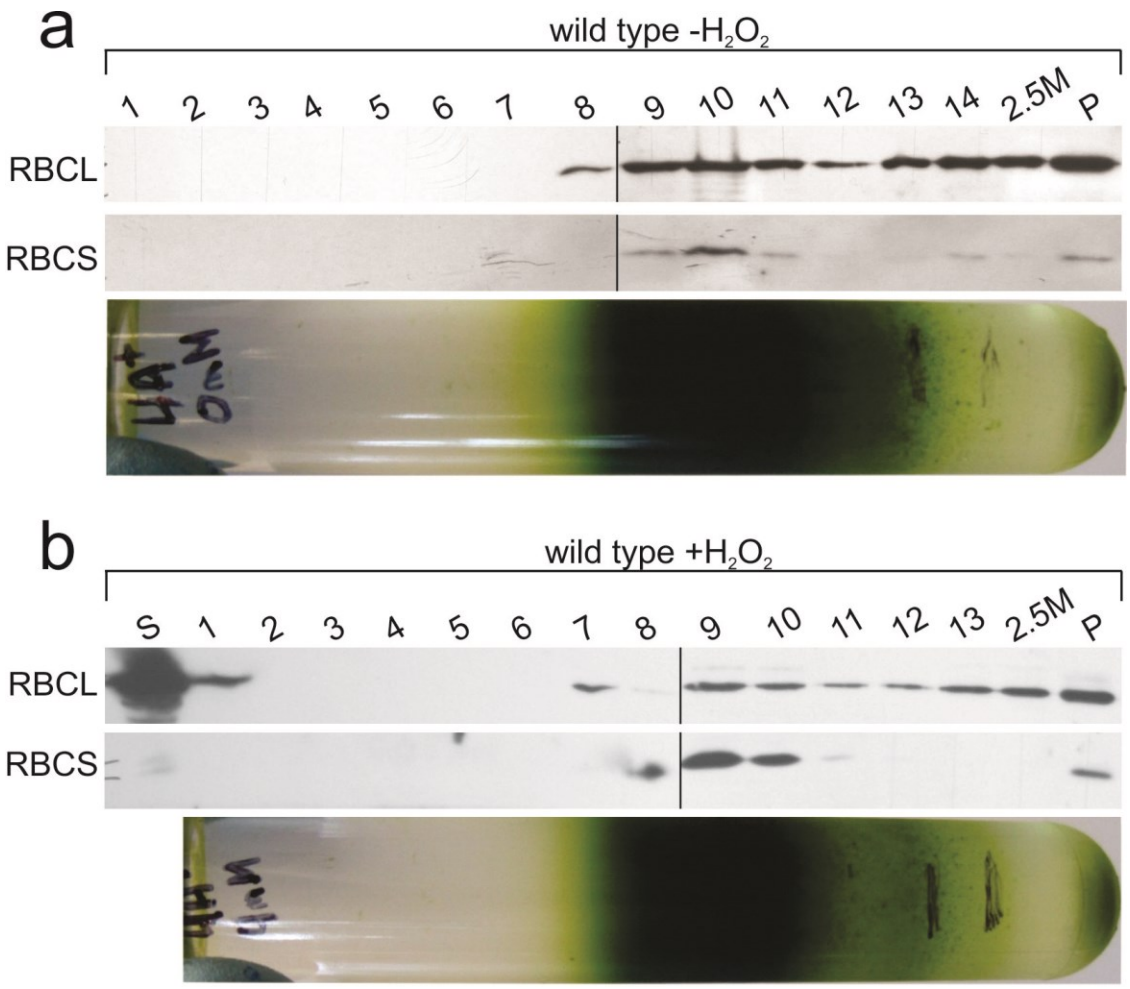

Figure 4) Subcellular fractionation revealed RBCL localization to membranes. Gradient fractions were examined from non-stressed wild type cells (a) and wild type cells exposed to 4 mM H_2O_2 (b). S indicates the supernatant from the initial high-speed fractionation (not shown in a). 2.5M indicates the sucrose solution from which the membranes were floated, meaning the gradients were centrifuged at 10^5 x g and membranes moved up into the gradient and banded according to their density. P indicates the pellet of the sucrose gradient. Each fraction was assayed for the presence of RBCL and RBCS. Black lines indicate where immunoblots of two gels were joined, for which all detection steps were carried out in the same conditions. The gradient fractions shown in panel a were provided by Dr. Marco Schottkowki.

not shown in Fig 4a). While fractions 7-10 were previously found to contain thylakoid membranes, the membranes of higher buoyant density in fraction 12-14 contain a novel compartment called the Chloroplast Translation Membrane (CTM). This compartment is hypothesized to be a site of active protein synthesis, where ribosomes and mRNAs are localized in close proximity to the import apparatus of the chloroplast envelope to co-ordinate the biogenesis of photosynthetic complexes (Schottkowski et al., 2012). In addition to co-localization with thylakoid membranes, it was intriguing that RBCL was also found in the CTM. In contrast, while RBCS was also detected in the thylakoid fractions, it did not similarly localize to the CTM (Fig. 4a). This suggests that if there is functional significance to RBCL localization to that compartment, it is independent of its role in Rubisco. However, despite the previously reported shift of Rubisco to membranes during oxidative stress, no change in the pattern of RBCL localization to the CTM was observed in lysates obtained from stressed wild type cells (Fig. 4b). It appears as though there is a change in the distribution of RBCL in fractions 7 and 8, following stress (Fig. 4b). However, this effect was not seen in all trials. Because these results are preliminary, further work must be done in order to determine whether this pattern was due to errors in manipulation or if it is reproducible. Finally, one would expect that if none of the RBCL in *ΔrbcS-dim1* is in Rubisco, then localizing the protein in this strain would reveal the site of its dual function. However, I was unable to detect any RBCL in membrane fractions obtained from *ΔrbcS-dim1* using this approach. This could be explained by my observation that *ΔrbcS-dim1* has only 1-2% of the wild-type amount of RBCL, and when separated across the 16-17 fractions generated, is below the detection threshold of immunoblot analysis. Alternatively, the detection of RBCL in *ΔrbcS-dim1* might be

obstructed by the presence of several cross-reacting proteins, which were detected strongly by the Rubisco holoenzyme antiserum that was used for this experiment.

In summary, the results of my analytical subcellular fractionation experiments revealed that in addition to the expected localization of RBCL to the supernatant in wild type, a minor amount also co-localized with a proposed membrane site for active mRNA translation. As RBCL is found in stress granules along with chloroplast mRNAs and small ribosomal subunits, these two compartments may share functional significance. It is important to note however, that these results are preliminary and are shown here for the purpose of documentation.

A minor pool of RBCL has altered biochemical properties

In order to further substantiate the existence of a dual function RBCL pool, as well as to characterize its properties, I took a second approach. Previous reports have shown that in addition to localizing to membranes under oxidizing conditions, RBCL disassembles from Rubisco, forms high molecular-weight aggregates, and is recruited to cpSGs (Marín-Navarro and Moreno, 2006; Uniacke and Zerges, 2008). Because little is known about the functional significance of Rubisco aggregation, and because SGs/cpSGs have never been characterized *in vitro*, I attempted to explore these previous observations in more detail. To this end, I developed a differential centrifugation scheme, in which fractions were collected from cell lysates following sequential increases in centrifugation speed, and the localization of marker proteins within the fractions were analyzed by Western blotting (Supplementary Fig. 3). Because cpSGs appear to be dense aggregates of protein and mRNA, I asked whether RBCL and other marker proteins for cpSGs might

have altered sedimentation properties following differential centrifugation, due to their recruitment to these structures. In addition to addressing these questions, these experiments were also intended to establish a reproducible procedure for studying the dual function RBCL pool in the future.

For my initial trials, I prepared lysates from cultures of wild-type and *ΔrbcS-dim1*, by cell breakage with a French press. Each lysate was first centrifuged for 1 minute at 3, 200 x g, and the pellet (P3) and supernatant (S3) were collected. S3 was then centrifuged for 20 min at 17, 000 x g, and the pellet (P17) and supernatant (S17) were collected. Finally, S17 was centrifuged for 1 hr at 100, 000 x g and the resulting pellet (P100) and supernatant (S100) were collected. In order to account for any material from the lysates that may have pelleted due to their association with membranes, or because they were trapped in vesicles following breakage, each pellet fraction was resuspended and treated with the detergent Triton X-100 to solubilize membranes. These pellet fractions were then centrifuged again at the same speeds at which they were initially recovered, to yield Triton-insoluble pellets (-TI) and Triton-soluble supernatants (-TS). Therefore, each cell lysate was separated into seven fractions: P3-TI, P3-TS, P17-TI, P17-TS, P100-TI, P100-TS, and S100. More dense material from the lysates is expected to pellet quickly, at low speed centrifugations, while less dense material is expected to require longer and faster centrifugation speeds to pellet.

As expected, in both wild type and *ΔrbcS-dim1* the S100 fraction contained a marker for the soluble chloroplast stroma, HSP70B (Supplementary Fig. 3). Some HSP70 pelleted following the initial low-speed centrifugations, as well as following ultracentrifugation, however in both cases it was mostly found in the triton-solubilized

pellets. This likely indicates that HSP70 pelleted either due to being trapped in unbroken cells, fragmented chloroplasts, or both. Indeed, upon examination with a light microscope, many unbroken cells were found in the P3 fraction. Ribosomal subunits in both strains were mostly found in the S100 fraction, as well as in P100-TI and P100-TS. The 30S and 50S ribosomal subunits in S100 are likely from monosomes, whereas those that pelleted (in both P100-TI and P100-TS) following ultracentrifugation are likely from translating polysomes, which were expected to associate with membranes (see description of the CTM, above). Additionally, the 30S subunit was also found in the fractions P3-TI and P17-TI, independently of the 50S subunit. Finally, I found that most RBCL in wild type remained in the S100 fraction, with minor amounts appearing in P3-TI, P17-TI, P100-TI, and P100-TS (Supplementary Fig. 3b). Because Rubisco is extremely abundant in wild type cells, it is possible that the presence of RBCL in the pellet fractions represents contamination from S100. In *ΔrbcS-dim1* however, RBCL was only detected in P17-TI. Because the P3 fraction contained unbroken cells, and because RBCL was not found in any of the fractions from *ΔrbcS-dim1*generated by ultracentrifugation, a more simplified centrifugation scheme was used for further analysis. In this scheme, fraction P3 was discarded, and the ultracentrifugation step was omitted. Therefore, in subsequent experiments, each cell lysate was separated into fractions P17-TI, P17-TS, and S17.

For this modified differential centrifugation experiment, I examined lysates from cultures of wild-type, *ΔrbcS-dim1*, and *ΔrbcL-MX3312* (Fig. 5). For wild type and *ΔrbcS-dim1*, the lysates were obtained both prior to and following exposure of the cultures to 4 mM H_2O_2 (Fig. 5a and b). As before, HSP70B was found in the soluble (S17) fraction,

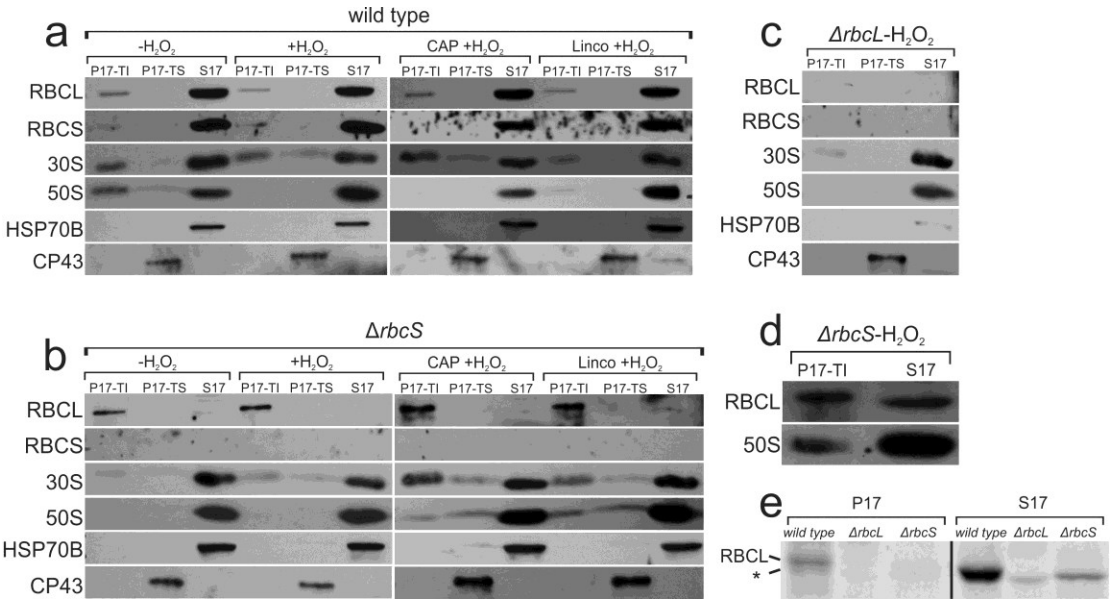

Figure 5) Differential Centrifugation revealed an extra-Rubisco subpool of RBCL.

a-d) RBCL localization during differential centrifugation and differential solubilisation with Triton X-100 was revealed by immunoblot analyses for a) the wild-type strain, b) *ΔrbcS-dim1*, and c) *ΔrbcL-MX3312.* Proteins analyzed were RBCL, RBCS, marker proteins for chloroplast ribosome subunits (30S and 50S), a soluble protein of the chloroplast (HSP70B), and an integral thylakoid membrane protein (CP43). S17 has soluble proteins, e.g. HSP70B. P17-TS has Triton-X100 soluble proteins, e.g. CP43. P17-TI has Triton-X100 insoluble proteins. Where indicated, fractions were prepared from cells that had been exposed to H_2O_2, chloramphenicol, or lincomycin (a, b). d) RBCL in P17-TI and S17 from the *ΔrbcS-dim1* strain differ slightly in electrophoretic mobility. To control for the specificity of this mobility difference for RBCL, the same blot was also immunoprobed for an r-protein of the 50S subunit of the chloroplast ribosome. e) ^{35}S pulse labelling of protein from wild type and *ΔrbcS-dim1* revealed that most newly-synthesized RBCL is in fraction S17. The S17 from *ΔrbcL* lacked ^{35}S-labelled RBCL but had an unknown ^{35}S-labelled protein of a slightly higher electrophoretic mobility, which

was also detected in certain fractions from the wild-type strain and *ΔrbcS* (asterisk). Panel e is cropped from the full length image shown in supplementary figure 5. The black line indicates where cropped images of the same exposure were joined.

along with the bulk of both the large and small ribosomal subunits. Fraction P17-TS was found to contain the CP43 subunit of photosystem II, a marker for thylakoid membranes, indicating that Triton-X100 efficiently solubilized membranes. As described in the previous section, some RBCL in wild type localized to both thylakoid membranes and the CTM. Therefore, it was unexpected that no RBCL in wild type was found in fraction P17-TI (Fig. 5a). As before, most RBCL in wild type was found in the supernatant (S17) fraction, while a minor amount pelleted following differential centrifugation and was present in P17-TI. Therefore, either the membranes to which RBCL localized as described in the previous section were not solubilized by Triton X-100, or else the RBCL found here in P17-TI is distinct from that found in membranes.

The RBCL of fraction P17-TI in wild type could not be distinguished from that of the Rubisco, because RBCS was also present in this fraction (Fig. 5a). This highlights the difficulty of identifying a dual function pool of RBCL in wild type amidst the background of the highly abundant Rubisco. The absence of Rubisco in *ΔrbcS-dim1* however, presumably meant that I could detect only the dual function pool of RBCL in this strain. In *ΔrbcS-dim1*, I found that only a minor amount of RBCL was detected in S17, while the vast majority of it was in the P17-TI fraction (Fig. 5b). This strongly suggests that a secondary form of RBCL exists in *ΔrbcS-dim1* that has altered sedimentation properties. This pool is presumed to also exist in wild type, because that strain also exhibited RBCL-dependant H_2O_2 tolerance; however it could not be distinguished from Rubisco-RBCL using this approach.

I also found that the RBCL in fraction P17-TI in *ΔrbcS-dim1* had a lower electrophoretic mobility than the RBCL found in fraction S17 (Fig. 5d). This result suggests that one or more of the many reported post-translational modifications to RBCL may be involved in its dual function (Houtz et al., 2008). While a size-shift was not obvious in the P17-TI RBCL from wild-type, it may again be the case that the abundant Rubisco pool of RBCL prevented its detection.

In addition to examining the state of the dual function pool of RBCL, I also asked whether it was possible to detect cpSGs using this approach. Because RBCL in *ΔrbcS-dim1* is found in P17-TI, and this strain presumably only contains the dual function of RBCL, I asked whether this fraction is enriched in markers for cpSGs. Several of the cpSG features (in addition to the presence of RBCL) that were previously characterized *in situ* were also tested here. First, as mentioned above, the 30S ribosomal subunit is recruited to cpSGs while the 50S subunit is not. When I probed the fractions obtained from the differential centrifugation of the lysates, I found that there was an increase in the proportion of 30S r-protein in P17-TI relative to the proportion of 50S r-protein there (Figure 5a and b). This can be seen in both the stressed wild type fractions, and in the *ΔrbcS-dim1* fractions. Overall, this effect was found in approximately 70% of the experimental replicates. The increase in the amount of 30S r-protein relative to 50S r-protein in P-17-TI was also found in *ΔrbcL-MX3312*, therefore it remains unclear if this effect is strictly due to the presence of cpSGs there (Fig. 5c). A second feature of cpSGs is that they only become visible following stress. For this reason, wild type and *ΔrbcS-dim1* lysates were fractionated and analyzed both prior to, and following treatment of cell cultures with H_2O_2, to test whether there were any significant changes in the distribution

of cpSG marker proteins following stress. However, in neither wild type or in *ΔrbcS-dim1* did I observe an increase in the amount of RBCL or 30S r-protein in fraction P17-TI following stress (Fig. 5a and b). There may appear to be a slight increase in the trial shown in Fig. 5, however this was not observed in the other four trials (data not shown). Nonetheless, this suggests that the dual function of the RBCL subpool that is required for H_2O_2-tolerance is present under both non-stress and stress conditions. This result suggests that RBCL functions in RNA homeostasis in addition to its putative role in cpSGs during oxidative stress. A third feature of cpSGs is that they exchange their mRNA components with polysomes on a minute time scale (Uniacke and Zerges, 2008). Treatment of *Chlamydomonas* with chloramphenicol arrests chloroplast translation by freezing polysomes on mRNAs, and this prevents the formation of cpSGs. On the other hand, lincomycin treatment clears polysomes from mRNAs, resulting in both increased cpSG formation during stress, and in the stabilization of pre-formed cpSGs during recovery. Therefore, I treated wild type and *ΔrbcS-dim1* cultures with either of these antibiotics prior to the addition of H_2O_2, and asked whether they had opposing effects on the distribution of cpSG marker proteins during differential centrifugation. However, as when I examined the effect of H_2O_2 treatment alone, I did not observe any significant effect of either antibiotic on the localization of RBCL or 30S r-proteins to fraction P17-TI, in either wild type or *ΔrbcS-dim1* cell lysates (Fig. 5a and b).

While this result did not further elucidate the presence of cpSGs in P17-TI, it might suggest that the RBCL found there is a stable pool, because the inhibition of chloroplast protein synthesis by chloramphenicol and lincomycin is thought to cause the degradation of Rubisco subunits (Chua and Gillham, 1977). Further support that RBCL in

P17-TI is a stable pool came when I examined the distribution of newly-synthesized proteins in wild type, *ΔrbcS-dim1* and *ΔrbcL-MX3312*. Fractions P17 and S17 were obtained from these strains following ^{35}S pulse labelling, and newly-synthesized RBCL was localized within them (Fig. 5e). I found that most of the newly-synthesized RBCL was in S17, for both wild type and *ΔrbcS-dim1*. This indicates that the RBCL that I detected in fraction P17-TI in *ΔrbcS-dim1* is not newly-synthesized.

In summary, the results of my differential centrifugation analysis have revealed that a secondary pool of RBCL exists in wild type and *ΔrbcS-dim1* that is likely responsible for the dual function of oxidative stress tolerance, and that this pool differs from the one found in Rubisco. This RBCL pool is not newly synthesized. Whether the RBCL pool characterized here differs from the membrane-localized form that I found earlier in wild type remains to be determined. Finally, I found that fraction P17-TI has some features that are consistent with cpSG composition, in that it contains RBCL and is enriched in 30S r-protein relative to 50S r-protein. It should be noted however, that the separation technique used here generates relatively crude fractions, the complexity of which can be seen in silver-stained gels (Fig. 6). Nonetheless, these experiments may provide an avenue for the eventual biochemical purification of cpSGs.

RBCL is not required for the mitigation of oxidative protein damage

Having established that a novel RBCL pool exists independently of Rubisco and is involved in oxidative stress tolerance, I next asked what the function of this pool might be. Because it was previously found that RBCL exists in cpSGs, and because these structures are aggregates of protein and mRNA, it was hypothesized that RBCL might

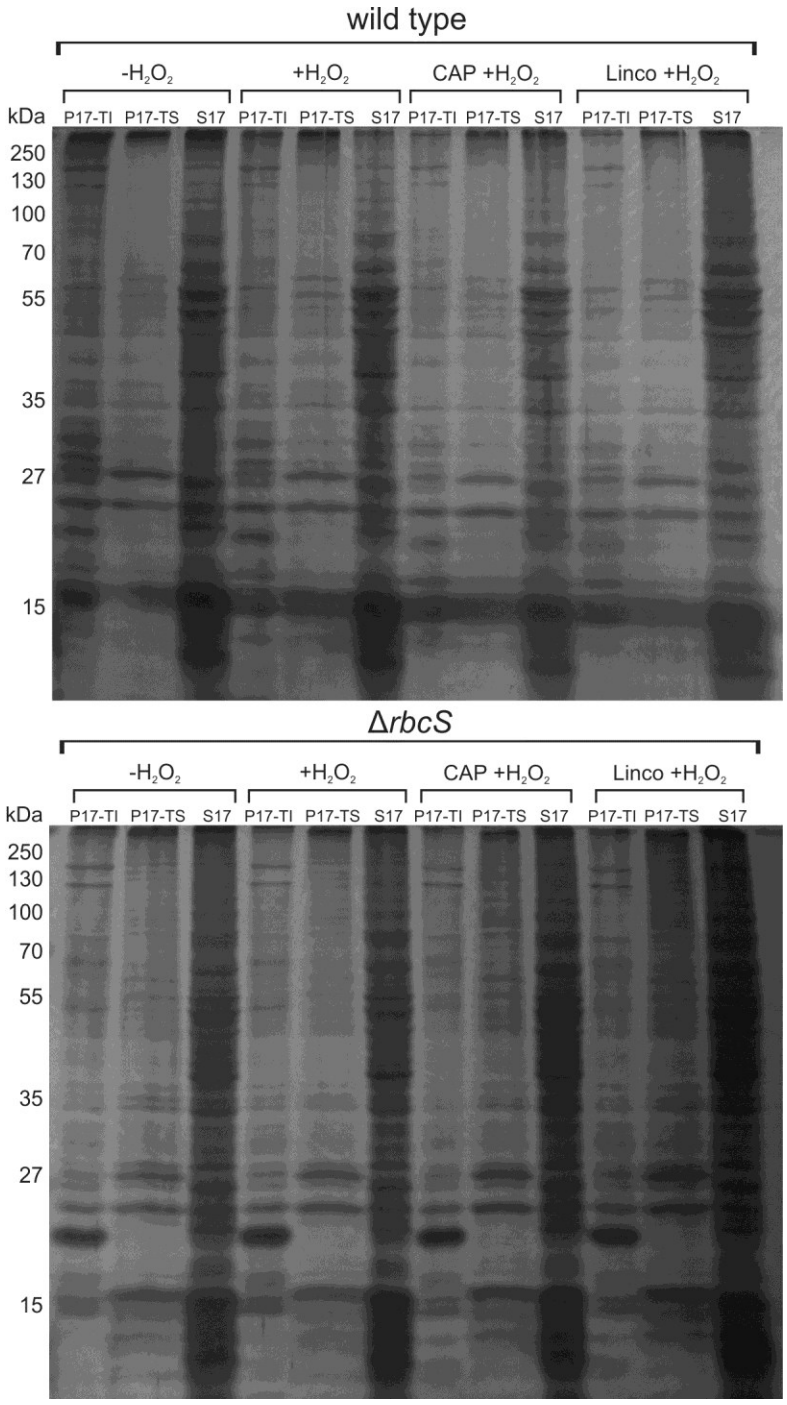

Figure 6) Silver Staining of Differential Centrifugation Fractions. The fractions shown in panels a and b from figure 5 were silver-stained to show the total protein within them (upper and lower panels, respectively). Molecular weight markers are shown on the left border of each image.

function in the control of damage to either protein or mRNA. Alternatively, RBCL might also be involved in the mitigation of oxidative damage to DNA or lipids. To this end, my colleague Yu Zhan and I examined the level of oxidative damage to biological molecules within wild type, *ΔrbcS-dim1*, and *ΔrbcL-MX3312*. Yu Zhan measured the amounts of oxidative damage to both total RNA and total DNA isolated from the aforementioned *Chlamydomonas* strains, while I attempted to measure the amounts of oxidative damage to both total protein and lipids. Our goal with these experiments was to determine if RBCL was required for the mitigation of damage to one or more of these biological molecules, and if so, if that requirement correlated with its role in oxidative stress tolerance and cpSG formation.

To examine the role of RBCL in the mitigation of oxidative damage to protein, I measured the amount of carbonylated amino acid residues in total protein extracts from wild type, *ΔrbcS-dim1*, and *ΔrbcL-MX3312*, by Western blotting. I analyzed protein extracts both prior to- and following exposure to H_2O_2, rose bengal, methyl viologen, UV-irradiation, and toxic metals (here, copper and cadmium) (Supplementary Fig. 4). Rose bengal and methyl viologen are photosensitizing dyes that cause $^1O_2$ and O_2^- production in the light, respectively (Baroli and Niyogi, 2003). Copper and cadmium exposure are also known to cause oxidative stress (Okamoto et al., 2001). I found that in each case, when RBCL was absent (in *ΔrbcL-MX3312*), there was no significant increase in the amount of carbonylated amino acid residues either prior to- or following- the exposure of the cells to the stressors. Furthermore, in contrast to when examining their survival in response to the addition of H_2O_2, *ΔrbcS-dim1* was not similarly *improved* in its response to the stresses. The amount of oxidative protein damage in each strain in

response to H_2O_2 was also represented graphically (Fig. 7). The ECL signals from carbonylated protein prior to and following stress were compared to the amount in *ΔrbcL-MX3312* prior to stress, since my question was whether wild type and *ΔrbcS-dim1* differ significantly from it. I found that under these conditions, *ΔrbcL-MX3312* is not impaired in oxidative protein damage, and furthermore, that the increase in protein carbonylation following stress was minimal. These results suggested that RBCL was not required for the mitigation of oxidative damage to proteins.

To analyze whether RBCL has a role in mitigating oxidative damage to lipids, I attempted to examine the amount of lipid peroxidation in the same cell lysates used for the examination of protein. The assay that I chose measures the amount of thiobarbituricacid reactive substances (TBARS), which include lipid peroxides. Unfortunately, the results that I obtained were inconclusive, as the amount of TBARS measured were irreproducible, and below the threshold of detection described by the assay kit used. Nonetheless, I was confident that under the same conditions used to analyze the other biological molecules, lipid peroxidation would not have been detectable because it was previously found that they only accumulate to measurable levels following 24 hrs of oxidative stress (Baroli et al., 2003).

In the case of RNA and DNA, a major indication of oxidative damage is the presence of 8-oxoG, an oxidatively modified form of guanosine. My colleague found that in comparisons of total RNA from wild type, *ΔrbcS-dim1*, and *ΔrbcL-MX3312* the level of 8-oxoG RNA in *ΔrbcL-MX3312* was significantly elevated (Yu Zhan, unpublished data). Furthermore, it was found that when compared to wild type, the amount of 8-oxoG RNA in *ΔrbcS-dim1* was significantly less. These effects were seen in non-stressed cells,

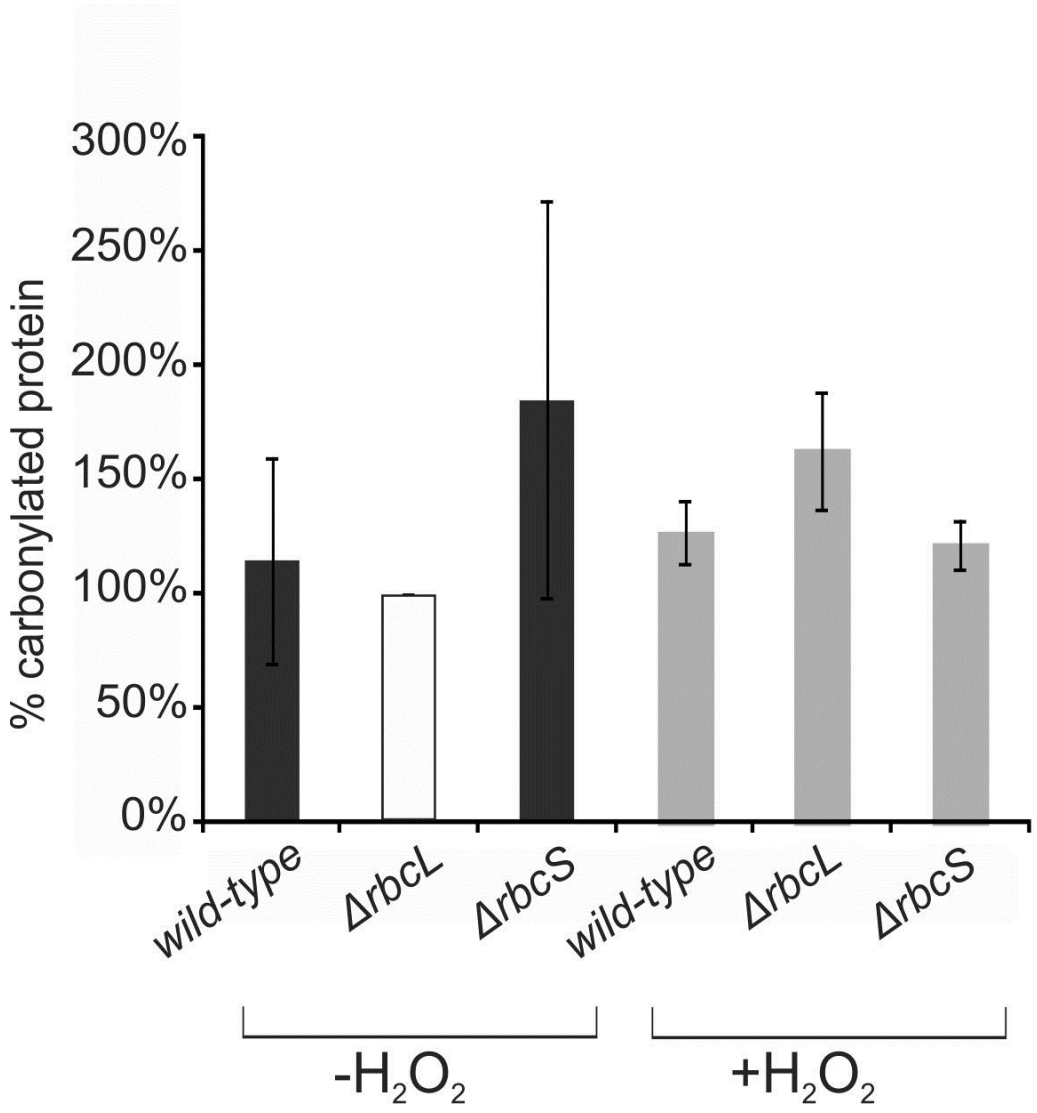

Figure 7) Oxidative protein damage is not controlled by RBCL. Oxidative damage to protein was determined as the relative levels of carbonylated amino acid residues in total protein from the strains indicated below the graph and determined under either non-stress condition (dark bars) (n=3) and following exposure to 2.0 mM H_2O_2 (grey bars) (n = 3) by immunoblot analysis (Supplementary Fig. 4). In each replicate, ECL signals were normalized to that of *ΔrbcL-MX3312* under the non-stress condition (designated as 100%) (white bar). Error bars indicate 1.0 standard error.

and did not appear to change following the addition of H_2O_2.These results indicated that in addition to its role in oxidative stress tolerance, RBCL was also required for the prevention of oxidative damage to RNA, independently of its function in Rubisco. When my colleague examined the amount of oxidative damage to DNA, it was found that RBCL was not similarly required for the prevention of oxidative damage, suggesting that its role may be specific to RNA (Yu Zhan, unpublished data).

In summary, in collaboration with my colleague, it was found that RBCL is specifically required for the mitigation or control of oxidative damage to RNA, and not to DNA, proteins, and probably not to lipids. RBCL was also found to exist in a minor, secondary pool that is required for oxidative stress tolerance, and therefore these results raise the possibility that the prevention of oxidative damage to RNAs by a dual function of RBCL is a major determinant of cell survival.

Heme staining of green native gels did not reveal an RBCL-dependant increase in redox-active metal

Having found that RBCL is both required for oxidative stress tolerance and for the mitigation of oxidative damage to RNA, I next asked whether these two phenotypes are linked, especially because little is known about the functional significance of oxidative RNA damage, as opposed to protein or DNA. As mentioned above, it was found that RBCL is required for the survival of *Chlamydomonas* following exposure to H_2O_2, and yet it is also required for the mitigation of RNA damage even under non-stress conditions. However, under these same non-stress conditions *ΔrbcL-MX3312* is able to grow normally, and does not have elevated transcripts for marker genes of oxidative

stress. (Yu Zhan, unpublished data). Therefore, it remained to be determined whether the RBCL-dependant impaired survival during oxidative stress is actually a consequence of RNA damage or not. In other words, how can elevated levels of RNA damage be tolerated during normal cell growth, yet become toxic only during exposure to exogenously added H_2O_2?

One possibility that was considered to answer this question was that oxidative RNA damage can lead to the production of misfolded proteins (Tanaka et al., 2007). In the chloroplast of *Chlamydomonas*, where RBCL is localized, most mRNAs transcribed from the chloroplast genome encode proteins of the photosynthetic electron transport chain, and several of these membrane-bound proteins are known to bind metal cofactors. Because Fe is a metal that is well known to participate in Fenton chemistry, in which the reaction of the metal with H_2O_2 leads to the production of more toxic ROS species such as $OH^{\cdot}$, it was hypothesized that when the proteins that bind them are misfolded, these metal cofactors may become more accessible to exogenously added H_2O_2. This could result in the increased production of intracellular ROS, which then leads to cell death.

In order to examine this possibility, I attempted to detect redox-active metals by in-gel heme staining of proteins obtained from wild type, *ΔrbcS-dim1*, and *ΔrbcL-MX3312*, both before and after exposure of the cells to H_2O_2. This technique is designed to specifically reveal the presence of proteins that contain the heme prosthetic group (Thomas et al., 1976). Although these experiments were ultimately unsuccessful, my intentions were to determine if there was a correlation between oxidative RNA damage and heme staining, and also to determine if RNA damage led to the increased staining of any specific heme-containing complexes. Therefore, lysates were obtained from cell

samples of the three strains both before and after exposure to H_2O_2, and membranes within them were analyzed by green-native PAGE (Fig. 8). Membranes from each sample were denatured by the addition of mild detergents, in a 20:1 detergent to chlorophyll ratio, as described previously (Allen and Staehelin, 1991). Green native PAGE and these denaturation conditions were chosen in order to preserve native heme-containing proteins or complexes, so that they may be detected in-gel. Following electrophoresis, each gel was stained with the compound TMBZ, which produces a blue colour due to the peroxidase activity of heme.

I found that most of the blue colour was at the bottom of the gel, in the low molecular weight ranges. This suggests that the denaturation conditions were too harsh to preserve native complexes. Cytochrome b_6 and cytochrome f of the Cytochrome b_6f complex are two heme-binding protein of the thylakoid membrane, with molecular weights of approximately 25 and 32 kDa, therefore the blue signal detected at the bottom of the gel could be from free Cytochrome b_6 or cytochrome f. Additionally, the blue staining could be due to free heme that was lost from heme-binding proteins during electrophoresis. I did not observe a significant difference in the TMBZ signal when RBCL was absent, in *ΔrbcL-MX3312*. However because I was unable to preserve native thylakoid membrane complexes with this method, I could not be sure whether there may be differences in heme staining of specific proteins or complexes.

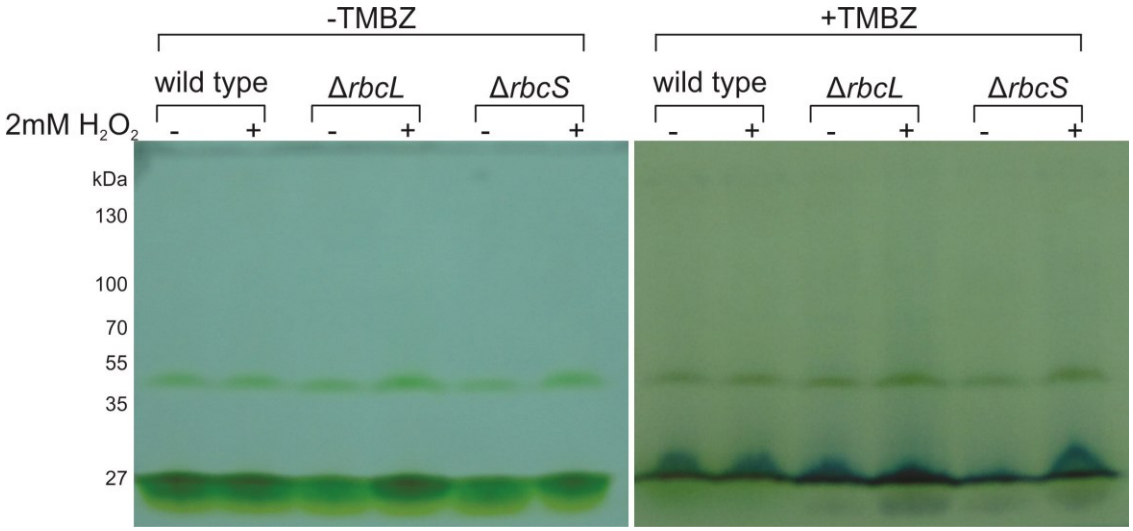

Figure 8) RBCL-dependant differences in peroxidase activity of hemeproteins were not observed by staining with TMBZ. Membranes from wild type, *ΔrbcL-MX3312*, and *ΔrbcS-dim1* were separated by Green-Native gel electrophoresis. Lysates were obtained from each strain both prior to- and following exposure to 2mM H_2O_2. The left image shows the unstained gel, and the right image shows the gel following TMBZ staining. Blue colour indicates the presence of peroxidase activity from heme groups. Molecular weight markers are shown on the left border.

Pulse labelling did not reveal an RBCL-dependant deficiency in protein synthesis

Because the result of my heme staining experiment was inconclusive in showing a link between RBCL-dependent oxidative RNA damage and impaired assembly of heme-containing proteins, that might lead to RBCL-dependent cell death, I took another approach. I asked whether protein synthesis in the chloroplast might be impaired or inhibited in the absence of RBCL, when oxidative RNA damage is elevated. Additionally, I asked whether there were specific proteins whose synthesis was impaired, which might indicate preferential oxidative damage to the mRNAs encoding them. To explore this hypothesis I performed ^{35}S pulse labelling, in which the total *de novo* protein synthesis amount in wild type, *ΔrbcS-dim1*, and *ΔrbcL-MX3312* was compared. Protein synthesis in each strain was examined both prior to, and following exposure to H_2O_2, and each cell sample was separated into fractions P17 and S17, in order to examine the synthesis of soluble and insoluble proteins separately (Supplementary Fig. 5). Unfortunately, the results of these experiments were inconclusive, and therefore this section serves to document the approach that was taken. Only a few bands were clearly resolved in each lane, and their ^{35}S labelling was not affected either between wild type and *ΔrbcL-MX3312*, or between *ΔrbcS-dim1*and *ΔrbcL-MX3312*. Therefore I was unable to determine if the RBCL deficiency affected the synthesis of any particular proteins.

Although I was unsuccessful in demonstrating a link between oxidative RNA damage and protein synthesis, the pulse labelling experiment nonetheless provided some insight into the location of newly-synthesized RBCL in wild type and in *ΔrbcS-dim1* (Fig. 5e).

Chapter 4: Discussion

Using a combination of genetic and biochemical approaches, I examined the properties of the large Rubisco subunit that contribute to its role in controlling oxidative stress tolerance. The results of my work revealed that a subpool of RBCL with altered biochemical properties is a major determinant in the survival of *Chlamydomonas reinhardtii* during exposure to exogenously added H_2O_2. The stress-tolerance function of this subpool of RBCL is independent of its role in photosynthesis. Due to RBCL localization to cpSGs, these observations may reflect a novel function of RNA granules during oxidative stress tolerance.

It was previously established that during oxidative stress, a *Chlamydomonas* mutant lacking RBCL (*ΔrbcL-MX3312)* is significantly impaired in both survival and viability, as compared to a wild type strain (Yu Zhan, unpublished data). *ΔrbcL-MX3312* lacks functional Rubisco and is non-photosynthetic. Its impaired oxidative stress tolerance reflects a role of RBCL and not Rubisco because *ΔrbcS-dim1*, which also lacks Rubisco but retains RBCL expression, is significantly improved in stress tolerance. The opposing phenotypes of these two mutants suggested that RBCL has a role in oxidative stress tolerance that is independent of its role in photosynthesis. I confirmed here that the stress tolerance phenotype of *ΔrbcS-dim1* was indeed RBCL-dependant because removing the gene encoding for it reduced survival and viability to the level of the *ΔrbcL-MX3312*. Furthermore, the observation that *ΔrbcS-dim1* has *improved* tolerance over wild type reveals that free RBCL is a key determinant in oxidative stress tolerance. When *ΔrbcS-dim1* was rescued by reinsertion of the *RBCS2* gene, its survival and viability were reduced to the level of the wild type strain (Fig. 2a and b). This suggests

that not only is RBCL required for stress tolerance, but that it has enhanced activity in the absence of its Rubisco assembly partner. Possible bases for this enhancement are discussed below.

Previous explorations of SG function have been limited for several reasons. Each of the proteins found in SGs also have functions in other cellular processes, and therefore any phenotypes observed following deletion or disruption of these components cannot be directly attributed to their recruitment to SGs. In addition, SGs have only been observed and studied microscopically, and further elucidation of their roles awaits their biochemical purification and *in vitro* reconstitution. The genetic approach used to examine RBCL in this study addresses both of these obstacles: The use of *ΔrbcS-dim1*, which lacks the primary RBCL function of photosynthesis, has allowed for the specific examination of the role of the RBCL subpool that functions in stress tolerance. The *ΔrbcS-dim1* mutant has also made it possible to identify a cellular subfraction that is enriched in this subpool, and therefore it is now possible that the continued purification of fraction P17-TI may lead to the isolation of intact cpSGs for further analysis.

The results of my biochemical analysis revealed that the stable, extra-Rubisco pool of RBCL has altered properties that may be consistent with its role as a stress response protein, and possibly with its recruitment to cpSGs (Fig. 5). Rubisco is a stroma-localized, soluble protein complex, and therefore, the localization of RBCL to the dense, insoluble P17-TI fraction may be due to its aggregation in cpSGs or similar mRNP assemblies. In addition, this fraction was also enriched in a marker for another component of cpSGs, the small subunit of the chloroplast ribosome. cpSGs are formed during stress when mRNAs are released from disassembling polysomes (Uniacke and

Zerges, 2008). Their formation is prevented when mRNAs are trapped on polysomes, and the release of mRNAs from polysomes by premature termination increases their formation and stability. When I treated *Chlamydomonas* cells with chloramphenicol or lincomycin prior to stress however, I did not observe opposing effects on RBCL localization to P17-TI, or in the distribution of 30S r-protein. Furthermore, I did not observe an increase in the localization of these markers to P17-TI in stressed cells. Finally, I found that RBCL localized to P17-TI even under non-stress conditions, when cpSGs are not observed. Therefore, it remains to be determined if RBCL localization to P17-TI is due to its assembly in cpSGs. One intriguing possibility is that cpSG-like assemblies constitutively forming during non-stress conditions, and that they only become microscopically visible during stress when there is an increase in available substrates from disassembling Rubisco and polysomes. This hypothesis remains to be explored for cytoplasmic SGs as well.

The slight shift in electrophoretic mobility that was observed in P17-TI RBCL suggests that it differs in conformation or in post-translational modification from that of Rubisco. There are many post-translational modifications reported for RBCL, and their functions have yet to be fully explored (Houtz et al., 2008). However, it has been suggested that the disassembly from Rubisco, RNA binding activity, and aggregation of RBCL are linked to redox regulation of its cysteine residues (Cohen et al., 2005; Moreno et al., 2008). Post-translational modifications are involved in the recruitment of several proteins to cytoplasmic SGs (Ohn and Anderson, 2010). Therefore, a future avenue for the study of cpSG function could be to explore whether interfering with known post-translational modifications of RBCL affects its localization to P17-TI or its stress-

tolerance function. This could be done by site-directed mutagenesis of the cysteine residues that are known to be involved in the redox regulation of RBCL RNA binding activity and Rubisco aggregation. Alternatively, the redox state of cysteine residues in the RBCL protein could be manipulated with the use of redox buffers such as cystamine and cysteamine (Moreno et al., 2008)

The extra-Rubisco function of RBCL during oxidative stress is clearly critical for the survival of *Chlamydomonas*. Because RBCL was previously found to bind RNA and localize to cpSGs during stress, it is possible that the survival phenotypes observed reflect its recruitment there. While the related SGs found in other eukaryotes have been hypothesized to sequester and control the translation of mRNAs during stress, we explored an alternate possibility that they may function in controlling molecular oxidative damage to the proteins or RNAs aggregated within them. My analysis of the mean level of carbonylated amino acids in total protein extracts of wild type, *ΔrbcL-MX3312*, and *ΔrbcS-dim1* exposed to H_2O_2 revealed that RBCL deficiency was not linked to increased protein oxidative damage (Fig. 7). While it has been suggested that oxidative damage to protein may contribute to the detrimental effects of oxidative stress, the amount of protein carbonylation observed here appeared to be variable even under non-stress conditions, and did not increase much following exposure to H_2O_2 under these experimental conditions. Previous reports in Arabidopsis and maize have shown that protein carbonylation varies greatly in controlled processes during development, suggesting that the link between oxidative protein damage and cell death is more complex than previously thought (Foyer and Noctor, 2009). When oxidative RNA damage was examined by my colleague, it was found that the mean level of 8-oxoG in total RNA

extracts was significantly increased in *ΔrbcL-MX3312*, as compared to wild type (Yu Zhan, unpublished data). It was also found that the level of 8-oxoG in *ΔrbcS-dim1* was significantly reduced below that of wild type. These results showed that RBCL has a role in the mitigation of oxidative RNA damage independently of its role in photosynthesis, and that this function is enhanced in the absence of its Rubisco assembly partner. It was confirmed that the reduced 8-oxoG RNA phenotype of *ΔrbcS-dim1* is RBCL-dependant because my colleague observed that the Δ*rbcL;*Δ*rbcS* strain that I created had elevated amounts of RNA damage, to the same level as *ΔrbcL-MX3312*. It also appears that when free of Rubisco, RBCL is better able to mitigate oxidative RNA damage because the rescue of *ΔrbcS-dim1* with *RBCS2* reversed its 8-oxoG RNA level to that of wild type.

The opposing levels of 8-oxoG in *ΔrbcL-MX3312* and *ΔrbcS-dim1* reveal that RBCL has a key function in controlling damage to RNA, in addition to being required for oxidative stress tolerance. This correlation suggests that the protection of RNA from oxidative damage is critical for the survival of *Chlamydomonas.* Intriguingly however, RBCL-dependant mitigation of RNA damage was observed prior to exposure of cells to H_2O_2. Because *ΔrbcL-MX3312* is able to grow normally, at the same rate as wild type and *ΔrbcS-dim1* (Yu Zhan, unpublished data), a direct link between oxidative RNA damage and cell death remained unclear. One possibility that might explain how RNA damage can accumulate without causing death, yet also lead to impaired tolerance to stress, is the nature of proteins encoded for by the damaged RNAs. Many of the chloroplast-encoded proteins that form the components of the photosynthetic electron transport chain bind metal cofactors. While these metals are normally tightly bound by their proteins, misfolding due to errors in translation caused by oxidative damage of the mRNAs

encoding them could lead to their misincorporation. Because Fe^{2+} can produce highly toxic $OH^{\cdot}$ radicals from H_2O_2, proteins with perturbed heme binding may predispose cells to death during oxidative stress (Ryter and Tyrrell, 2000). I attempted to determine whether the RBCL deficiency and increased level of 8-oxoG RNA of *ΔrbcL-MX3312* correlated with perturbed heme binding, however the results were inconclusive. Nonetheless, the fact that H_2O_2 and other ROS are constantly produced by the photosynthetic electron transport chain suggests that the accumulation of misfolded proteins with accessible redox-active metals is detrimental to cell fitness. Another way to address this issue might be to examine whether the synthesis of specific proteins, perhaps those that bind to metal cofactors, is affected by RBCL deficiency. However, my attempts to examine specific deficiencies in protein synthesis by ^{35}S pulse labelling were unsuccessful.

The importance for the mitigation of RNA oxidative damage might also be reflected by the localization of RBCL in wild type to membrane fractions that overlap with CTMs. This compartment is proposed to specialize in protein synthesis, with the ribosomes and other translation factors of the chloroplast genetic system localizing there for the biogenesis of the photosynthetic protein complexes of the thylakoid membrane (Schottkowski et al., 2012). Therefore, the mRNAs and translation machinery in this compartment are in close proximity to the ROS-generating photosynthetic electron transport chain, and RBCL might be localized there to meet disassembling polysomes for cpSG formation and mitigation of oxidative damage to the mRNAs. Although I was unable to detect RBCL from *ΔrbcS-dim1* in these fractions, it will be interesting to examine CTMs further in the context of the stress-function of RBCL.

How is it possible that *ΔrbcS-dim1* is enhanced over wild type in both stress tolerance and RNA damage phenotypes? In wild type, RBCL is normally assembled with RBCS in the Rubisco holoenzyme in the pyrenoid. During stress, Rubisco is disassembled and RBCL is released, presumably to function as a stress response protein. It is possible then, that in *ΔrbcS-dim1*, when it is not assembled in Rubisco, RBCL is more rapidly able to bind RNA for its dual function. The reversal of both the high stress tolerance and low 8-oxoG RNA phenotypes of *ΔrbcS-dim1* when *RBCS2* was introduced supports the idea that RBCL is more able to perform its stress function when not sequestered in Rubisco. Because it appears that only 1-2% of the wild type amount of RBCL is sufficient for the enhanced survival of *ΔrbcS-dim1*, one might ask why a dedicated pool of RBCL that is free from Rubisco is not maintained in wild type cells for this dual function. It is important to note however, that the conditions in which we observed the dual function of RBCL in stress tolerance are extreme, and would not be encountered by wild type *Chlamydomonas* in nature. Therefore, maintaining the level of dual-function RBCL activity of *ΔrbcS-dim1*during physiological conditions may not be beneficial. Therefore, our hypothesis is that two pools of RBCL exist. One that is in Rubisco for photosynthesis and another that protects RNA from damage and is required for stress tolerance. Because RBCL-dependant mitigation of RNA damage was observed prior to stress, the secondary pool of Rubisco is presumed to exist under non-stress conditions. This was substantiated by my finding that a stable subpool of non-Rubisco RBCL exists under non-stress conditions. Because cpSGs are not detected in most cells prior to stress, this second RBCL pool could exist in submicroscopic RNPs throughout the chloroplast, which only become visible during stress.

References

Allen, J.F., and Raven, J.A. (1996). Free-radical-induced mutation vs redox regulation: costs and benefits of genes in organelles. J. Mol. Evol. *42*, 482–492.

Allen, K.D., and Staehelin, L.A. (1991). Resolution of 16 to 20 chlorophyll-protein complexes using a low ionic strength native green gel system. Anal. Biochem. *194*, 214–222.

Anderson, P., and Kedersha, N. (2008). Stress granules: the Tao of RNA triage. Trends Biochem. Sci. *33*, 141–150.

Apel, K., and Hirt, H. (2004). Reactive oxygen species: metabolism, oxidative stress, and signal transduction. Annu. Rev. Plant Biol. *55*, 373–399.

Asada, K. (2000). The water-water cycle as alternative photon and electron sinks. Philos. Trans. R. Soc. Lond. B. Biol. Sci. *355*, 1419–1431.

Baroli, I., and Niyogi, K. (2003). Photo-oxidative Stress in a Xanthophyll-deficient Mutant of Chlamydomonas. J. Biol. Chem. *279*, 6337–6344.

Baroli, I., Do, A.D., Yamane, T., and Niyogi, K.K. (2003). Zeaxanthin accumulation in the absence of a functional xanthophyll cycle protects Chlamydomonas reinhardtii from photooxidative stress. Plant Cell *15*, 992–1008.

Boynton, J.E., and Gillham, N.W. (1993). Chloroplast transformation in Chlamydomonas. Methods Enzymol. *217*, 510–536.

Buchan, J.R., and Parker, R. (2009). Eukaryotic stress granules: the ins and outs of translation. Mol. Cell *36*, 932–941.

Choquet, Y., Zito, F., Wostrikoff, K., and Wollman, F.-A. (2003). Cytochrome f translation in Chlamydomonas chloroplast is autoregulated by its carboxyl-terminal domain. Plant Cell *15*, 1443–1454.

Chua, N.H., and Gillham, N.W. (1977). The sites of synthesis of the principal thylakoid membrane polypeptides in Chlamydomonas reinhardtii. J. Cell Biol. *74*, 441–452.

Cieśla, J. (2006). Metabolic enzymes that bind RNA: yet another level of cellular regulatory network? Acta Biochim. Pol. *53*, 11–32.

Cohen, I., Knopf, J.A., Irihimovitch, V., and Shapira, M. (2005). A proposed mechanism for the inhibitory effects of oxidative stress on Rubisco assembly and its subunit expression. Plant Physiol. *137*, 738–746.

Cohen, I., Sapir, Y., and Shapira, M. (2006). A conserved mechanism controls translation of Rubisco large subunit in different photosynthetic organisms. Plant Physiol. *141*, 1089–1097.

Dent, R.M., Haglund, C.M., Chin, B.L., Kobayashi, M.C., and Niyogi, K.K. (2005). Functional genomics of eukaryotic photosynthesis using insertional mutagenesis of Chlamydomonas reinhardtii. Plant Physiol. *137*, 545–556.

Ellis, R. (1979). The Most Abundant Protein in the World. Trends Biochem. Sci. *4*, 241–244.

Elzinga, S.D., Bednarz, A.L., van Oosterum, K., Dekker, P.J., and Grivell, L.A. (1993). Yeast mitochondrial NAD(+)-dependent isocitrate dehydrogenase is an RNA-binding protein. Nucleic Acids Res. *21*, 5328–5331.

Escoubas, J.M., Lomas, M., LaRoche, J., and Falkowski, P.G. (1995). Light intensity regulation of cab gene transcription is signaled by the redox state of the plastoquinone pool. Proc. Natl. Acad. Sci. U. S. A. *92*, 10237–10241.

Fischer, B.B., Hideg, É., and Krieger-Liszkay, A. (2013). Production, detection, and signaling of singlet oxygen in photosynthetic organisms. Antioxidants Redox Signal. *18*, 2145–2162.

Foyer, C.H., and Noctor, G. (2009). Redox regulation in photosynthetic organisms: signaling, acclimation, and practical implications. Antioxidants Redox Signal. *11*, 861–905.

Foyer, C.H., and Shigeoka, S. (2011). Understanding oxidative stress and antioxidant functions to enhance photosynthesis. Plant Physiol. *155*, 93–100.

Garg, N., and Manchanda, G. (2009). ROS generation in plants: Boon or bane? Plant Biosyst. - Int. J. Deal. Asp. Plant Biol. *143*, 81–96.

Ghezzi, P., and Bonetto, V. (2003). Redox proteomics: identification of oxidatively modified proteins. Proteomics *3*, 1145–1153.

Gilks, N., Kedersha, N., Ayodele, M., Shen, L., Stoecklin, G., Dember, L.M., and Anderson, P. (2004). Stress granule assembly is mediated by prion-like aggregation of TIA-1. Mol. Biol. Cell *15*, 5383–5398.

Gill, S.S., and Tuteja, N. (2010). Reactive oxygen species and antioxidant machinery in abiotic stress tolerance in crop plants. Plant Physiol. Biochem. PPB Société Française Physiol. Végétale *48*, 909–930.

Girotti, A.W., and Kriska, T. (2004). Role of lipid hydroperoxides in photo-oxidative stress signaling. Antioxidants Redox Signal. *6*, 301–310.

Harding, H.P., Zhang, Y., Bertolotti, A., Zeng, H., and Ron, D. (2000). Perk is essential for translational regulation and cell survival during the unfolded protein response. Mol. Cell *5*, 897–904.

Harris, E.H. (1989). The Chlamydomonas Sourcebook. A Comprehensive Guide to Biology and Laboratory Use. Elizabeth H. Harris. Academic Press, San Diego, CA, 1989. xiv, 780 pp., illus. $145. Science *246*, 1503–1504.

Hayakawa, H., Kuwano, M., and Sekiguchi, M. (2001). Specific binding of 8-oxoguanine-containing RNA to polynucleotide phosphorylase protein. Biochemistry (Mosc.) *40*, 9977–9982.

Hayakawa, H., Uchiumi, T., Fukuda, T., Ashizuka, M., Kohno, K., Kuwano, M., and Sekiguchi, M. (2002). Binding capacity of human YB-1 protein for RNA containing 8-oxoguanine. Biochemistry (Mosc.) *41*, 12739–12744.

Hernández-Pérez, L., Depardón, F., Fernández- Ramírez, F., Sánchez-Trujillo, A., Bermúdez-Crúz, R.M., Dangott, L., and Montañez, C. (2011). α-Enolase binds to RNA. Biochimie *93*, 1520–1528.

Higgs, D.C. (2009). The Chloroplast Genome. In The Chlamydomonas Sourcebook, (Elsevier), pp. 871–891.

Hofer, T., Badouard, C., Bajak, E., Ravanat, J.-L., Mattsson, A., and Cotgreave, I.A. (2005). Hydrogen peroxide causes greater oxidation in cellular RNA than in DNA. Biol. Chem. *386*, 333–337.

Holt, N.E., Fleming, G.R., and Niyogi, K.K. (2004). Toward an understanding of the mechanism of nonphotochemical quenching in green plants. Biochemistry (Mosc.) *43*, 8281–8289.

Honda, K., Smith, M.A., Zhu, X., Baus, D., Merrick, W.C., Tartakoff, A.M., Hattier, T., Harris, P.L., Siedlak, S.L., Fujioka, H., et al. (2005). Ribosomal RNA in Alzheimer disease is oxidized by bound redox-active iron. J. Biol. Chem. *280*, 20978–20986.

Houtz, R.L., Magnani, R., Nayak, N.R., and Dirk, L.M.A. (2008). Co- and post-translational modifications in Rubisco: unanswered questions. J. Exp. Bot. *59*, 1635–1645.

Hoyle, N.P., Castelli, L.M., Campbell, S.G., Holmes, L.E.A., and Ashe, M.P. (2007). Stress-dependent relocalization of translationally primed mRNPs to cytoplasmic granules that are kinetically and spatially distinct from P-bodies. J. Cell Biol. *179*, 65–74.

Imlay, J.A., and Linn, S. (1988). DNA damage and oxygen radical toxicity. Science *240*, 1302–1309.

Johnson, X., Wostrikoff, K., Finazzi, G., Kuras, R., Schwarz, C., Bujaldon, S., Nickelsen, J., Stern, D.B., Wollman, F.-A., and Vallon, O. (2010). MRL1, a conserved Pentatricopeptide repeat protein, is required for stabilization of rbcL mRNA in Chlamydomonas and Arabidopsis. Plant Cell *22*, 234–248.

Kasahara, M., Kagawa, T., Oikawa, K., Suetsugu, N., Miyao, M., and Wada, M. (2002). Chloroplast avoidance movement reduces photodamage in plants. Nature *420*, 829–832.

Kedersha, N., Cho, M.R., Li, W., Yacono, P.W., Chen, S., Gilks, N., Golan, D.E., and Anderson, P. (2000). Dynamic shuttling of TIA-1 accompanies the recruitment of mRNA to mammalian stress granules. J. Cell Biol. *151*, 1257–1268.

Kedersha, N., Chen, S., Gilks, N., Li, W., Miller, I.J., Stahl, J., and Anderson, P. (2002). Evidence that ternary complex (eIF2-GTP-tRNA(i)(Met))-deficient preinitiation complexes are core constituents of mammalian stress granules. Mol. Biol. Cell *13*, 195–210.

Kedersha, N.L., Gupta, M., Li, W., Miller, I., and Anderson, P. (1999). RNA-binding proteins TIA-1 and TIAR link the phosphorylation of eIF-2 alpha to the assembly of mammalian stress granules. J. Cell Biol. *147*, 1431–1442.

Kehrer, J.P. (2000). The Haber-Weiss reaction and mechanisms of toxicity. Toxicology *149*, 43–50.

Khrebtukova, I., and Spreitzer, R.J. (1996). Elimination of the Chlamydomonas gene family that encodes the small subunit of ribulose-1,5-bisphosphate carboxylase/oxygenase. Proc. Natl. Acad. Sci. U. S. A. *93*, 13689–13693.

Kimball, S.R., Horetsky, R.L., Ron, D., Jefferson, L.S., and Harding, H.P. (2003). Mammalian stress granules represent sites of accumulation of stalled translation initiation complexes. Am. J. Physiol. Cell Physiol. *284*, C273–284.

Kindle, K.L. (1990). High-frequency nuclear transformation of Chlamydomonas reinhardtii. Proc. Natl. Acad. Sci. U. S. A. *87*, 1228–1232.

Klausner, R.D., and Rouault, T.A. (1993). A double life: cytosolic aconitase as a regulatory RNA binding protein. Mol. Biol. Cell *4*, 1–5.

Knopf, J.A., and Shapira, M. (2005). Degradation of Rubisco SSU during oxidative stress triggers aggregation of Rubisco particles in Chlamydomonas reinhardtii. Planta *222*, 787–793.

Laemmli, U.K. (1970). Cleavage of structural proteins during the assembly of the head of bacteriophage T4. Nature *227*, 680–685.

Ledford, H.K., and Niyogi, K.K. (2005). Singlet oxygen and photo-oxidative stress management in plants and algae. Plant Cell Environ. *28*, 1037–1045.

Li, Z., Wu, J., and Deleo, C.J. (2006). RNA damage and surveillance under oxidative stress. IUBMB Life *58*, 581–588.

Li, Z., Keasling, J.D., and Niyogi, K.K. (2012). Overlapping photoprotective function of vitamin E and carotenoids in Chlamydomonas. Plant Physiol. *158*, 313–323.

Liu, X., Kim, C.N., Yang, J., Jemmerson, R., and Wang, X. (1996). Induction of apoptotic program in cell-free extracts: requirement for dATP and cytochrome c. Cell *86*, 147–157.

Marín-Navarro, J., and Moreno, J. (2006). Cysteines 449 and 459 modulate the reduction-oxidation conformational changes of ribulose 1.5-bisphosphate carboxylase/oxygenase and the translocation of the enzyme to membranes during stress. Plant Cell Environ. *29*, 898–908.

Mazroui, R., Sukarieh, R., Bordeleau, M.-E., Kaufman, R.J., Northcote, P., Tanaka, J., Gallouzi, I., and Pelletier, J. (2006). Inhibition of ribosome recruitment induces stress granule formation independently of eukaryotic initiation factor 2alpha phosphorylation. Mol. Biol. Cell *17*, 4212–4219.

McEwen, E., Kedersha, N., Song, B., Scheuner, D., Gilks, N., Han, A., Chen, J.-J., Anderson, P., and Kaufman, R.J. (2005). Heme-regulated inhibitor kinase-mediated phosphorylation of eukaryotic translation initiation factor 2 inhibits translation, induces stress granule formation, and mediates survival upon arsenite exposure. J. Biol. Chem. *280*, 16925–16933.

McKay, R.M.L., and Gibbs, S.P. (1991). Composition and function of pyrenoids: cytochemical and immunocytochemical approaches. Can. J. Bot. *69*, 1040–1052.

Mehta, R.A., Fawcett, T.W., Porath, D., and Mattoo, A.K. (1992). Oxidative stress causes rapid membrane translocation and in vivo degradation of ribulose-1,5-bisphosphate carboxylase/oxygenase. J. Biol. Chem. *267*, 2810–2816.

Meskauskiene, R., Nater, M., Goslings, D., Kessler, F., op den Camp, R., and Apel, K. (2001). FLU: a negative regulator of chlorophyll biosynthesis in Arabidopsis thaliana. Proc. Natl. Acad. Sci. U. S. A. *98*, 12826–12831.

Minai, L., Wostrikoff, K., Wollman, F.-A., and Choquet, Y. (2006). Chloroplast biogenesis of photosystem II cores involves a series of assembly-controlled steps that regulate translation. Plant Cell *18*, 159–175.

Miziorko, H.M., and Lorimer, G.H. (1983). Ribulose-1,5-bisphosphate carboxylase-oxygenase. Annu. Rev. Biochem. *52*, 507–535.

Mokas, S., Mills, J.R., Garreau, C., Fournier, M.-J., Robert, F., Arya, P., Kaufman, R.J., Pelletier, J., and Mazroui, R. (2009). Uncoupling stress granule assembly and translation initiation inhibition. Mol. Biol. Cell *20*, 2673–2683.

Moreno, J., García-Murria, M.J., and Marín-Navarro, J. (2008). Redox modulation of Rubisco conformation and activity through its cysteine residues. J. Exp. Bot. *59*, 1605–1614.

Murata, N., Takahashi, S., Nishiyama, Y., and Allakhverdiev, S.I. (2007). Photoinhibition of photosystem II under environmental stress. Biochim. Biophys. Acta *1767*, 414–421.

Murray, M.G., and Thompson, W.F. (1980). Rapid isolation of high molecular weight plant DNA. Nucleic Acids Res. *8*, 4321–4325.

Nagy, E., and Rigby, W.F. (1995). Glyceraldehyde-3-phosphate dehydrogenase selectively binds AU-rich RNA in the NAD(+)-binding region (Rossmann fold). J. Biol. Chem. *270*, 2755–2763.

Nishiyama, Y., Yamamoto, H., Allakhverdiev, S.I., Inaba, M., Yokota, A., and Murata, N. (2001). Oxidative stress inhibits the repair of photodamage to the photosynthetic machinery. EMBO J. *20*, 5587–5594.

Nover, L., Scharf, K.D., and Neumann, D. (1983). Formation of cytoplasmic heat shock granules in tomato cell cultures and leaves. Mol. Cell. Biol. *3*, 1648–1655.

Nover, L., Scharf, K.D., and Neumann, D. (1989). Cytoplasmic heat shock granules are formed from precursor particles and are associated with a specific set of mRNAs. Mol. Cell. Biol. *9*, 1298–1308.

Nunomura, A., Honda, K., Takeda, A., Hirai, K., Zhu, X., Smith, M.A., and Perry, G. (2006). Oxidative damage to RNA in neurodegenerative diseases. J. Biomed. Biotechnol. *2006*, 82323.

Ohn, T., and Anderson, P. (2010). The role of posttranslational modifications in the assembly of stress granules. Wiley Interdiscip. Rev. RNA *1*, 486–493.

Okamoto, O.K., Pinto, E., Latorre, L.R., Bechara, E.J., and Colepicolo, P. (2001). Antioxidant modulation in response to metal-induced oxidative stress in algal chloroplasts. Arch. Environ. Contam. Toxicol. *40*, 18–24.

Park, E.M., Shigenaga, M.K., Degan, P., Korn, T.S., Kitzler, J.W., Wehr, C.M., Kolachana, P., and Ames, B.N. (1992). Assay of excised oxidative DNA lesions: isolation of 8-oxoguanine and its nucleoside derivatives from biological fluids with a monoclonal antibody column. Proc. Natl. Acad. Sci. U. S. A. *89*, 3375–3379.

Pioli, P.A., Hamilton, B.J., Connolly, J.E., Brewer, G., and Rigby, W.F.C. (2002). Lactate dehydrogenase is an AU-rich element-binding protein that directly interacts with AUF1. J. Biol. Chem. *277*, 35738–35745.

Porra, R.J. (2002). The chequered history of the development and use of simultaneous equations for the accurate determination of chlorophylls a and b. Photosynth. Res. *73*, 149–156.

Rochaix, J.-D. (2011). Regulation of photosynthetic electron transport. Biochim. Biophys. Acta *1807*, 375–383.

Ryter, S.W., and Tyrrell, R.M. (2000). The heme synthesis and degradation pathways: role in oxidant sensitivity. Heme oxygenase has both pro- and antioxidant properties. Free Radic. Biol. Med. *28*, 289–309.

Satagopan, S., and Spreitzer, R.J. (2004). Substitutions at the Asp-473 latch residue of chlamydomonas ribulosebisphosphate carboxylase/oxygenase cause decreases in carboxylation efficiency and CO(2)/O(2) specificity. J. Biol. Chem. *279*, 14240–14244.

Schottkowski, M., Peters, M., Zhan, Y., Rifai, O., Zhang, Y., and Zerges, W. (2012). Biogenic membranes of the chloroplast in Chlamydomonas reinhardtii. Proc. Natl. Acad. Sci. U. S. A. *109*, 19286–19291.

Shao, N., Beck, C.F., Lemaire, S.D., and Krieger-Liszkay, A. (2008). Photosynthetic electron flow affects H2O2 signaling by inactivation of catalase in Chlamydomonas reinhardtii. Planta *228*, 1055–1066.

Spreitzer, R.J., and Salvucci, M.E. (2002). Rubisco: structure, regulatory interactions, and possibilities for a better enzyme. Annu. Rev. Plant Biol. *53*, 449–475.

Srivastava, S.P., Kumar, K.U., and Kaufman, R.J. (1998). Phosphorylation of eukaryotic translation initiation factor 2 mediates apoptosis in response to activation of the double-stranded RNA-dependent protein kinase. J. Biol. Chem. *273*, 2416–2423.

Stadtman, E.R., and Berlett, B.S. (1997). Reactive oxygen-mediated protein oxidation in aging and disease. Chem. Res. Toxicol. *10*, 485–494.

Strober, W. (2001). Trypan Blue Exclusion Test of Cell Viability. In Current Protocols in Immunology, J.E. Coligan, B.E. Bierer, D.H. Margulies, E.M. Shevach, and W. Strober, eds. (Hoboken, NJ, USA: John Wiley & Sons, Inc.),.

Takahashi, S., and Murata, N. (2008). How do environmental stresses accelerate photoinhibition? Trends Plant Sci. *13*, 178–182.

Tanaka, M., Chock, P.B., and Stadtman, E.R. (2007). Oxidized messenger RNA induces translation errors. Proc. Natl. Acad. Sci. U. S. A. *104*, 66–71.

Thomas, P.E., Ryan, D., and Levin, W. (1976). An improved staining procedure for the detection of the peroxidase activity of cytochrome P-450 on sodium dodecyl sulfate polyacrylamide gels. Anal. Biochem. *75*, 168–176.

Tourrière, H., Gallouzi, I.E., Chebli, K., Capony, J.P., Mouaikel, J., van der Geer, P., and Tazi, J. (2001). RasGAP-associated endoribonuclease G3Bp: selective RNA degradation and phosphorylation-dependent localization. Mol. Cell. Biol. *21*, 7747–7760.

Tuteja, N., Ahmad, P., Panda, B.B., and Tuteja, R. (2009). Genotoxic stress in plants: shedding light on DNA damage, repair and DNA repair helicases. Mutat. Res. *681*, 134–149.

Uniacke, J., and Zerges, W. (2007). Photosystem II assembly and repair are differentially localized in Chlamydomonas. Plant Cell *19*, 3640–3654.

Uniacke, J., and Zerges, W. (2008). Stress induces the assembly of RNA granules in the chloroplast of Chlamydomonas reinhardtii. J. Cell Biol. *182*, 641–646.

Uniacke, J., and Zerges, W. (2009). Chloroplast protein targeting involves localized translation in Chlamydomonas. Proc. Natl. Acad. Sci. U. S. A. *106*, 1439–1444.

Weber, C., Nover, L., and Fauth, M. (2008). Plant stress granules and mRNA processing bodies are distinct from heat stress granules. Plant J. Cell Mol. Biol. *56*, 517–530.

Wostrikoff, K., Girard-Bascou, J., Wollman, F.-A., and Choquet, Y. (2004). Biogenesis of PSI involves a cascade of translational autoregulation in the chloroplast of Chlamydomonas. EMBO J. *23*, 2696–2705.

Wu, J., and Li, Z. (2008). Human polynucleotide phosphorylase reduces oxidative RNA damage and protects HeLa cell against oxidative stress. Biochem. Biophys. Res. Commun. *372*, 288–292.

Wu, J., Jiang, Z., Liu, M., Gong, X., Wu, S., Burns, C.M., and Li, Z. (2009). Polynucleotide phosphorylase protects Escherichia coli against oxidative stress. Biochemistry (Mosc.) *48*, 2012–2020.

Wurtmann, E.J., and Wolin, S.L. (2009). RNA under attack: cellular handling of RNA damage. Crit. Rev. Biochem. Mol. Biol. *44*, 34–49.

Yosef, I., Irihimovitch, V., Knopf, J.A., Cohen, I., Orr-Dahan, I., Nahum, E., Keasar, C., and Shapira, M. (2004). RNA binding activity of the ribulose-1,5-bisphosphate carboxylase/oxygenase large subunit from Chlamydomonas reinhardtii. J. Biol. Chem. *279*, 10148–10156.

Appendix 1-Supplementary Figures

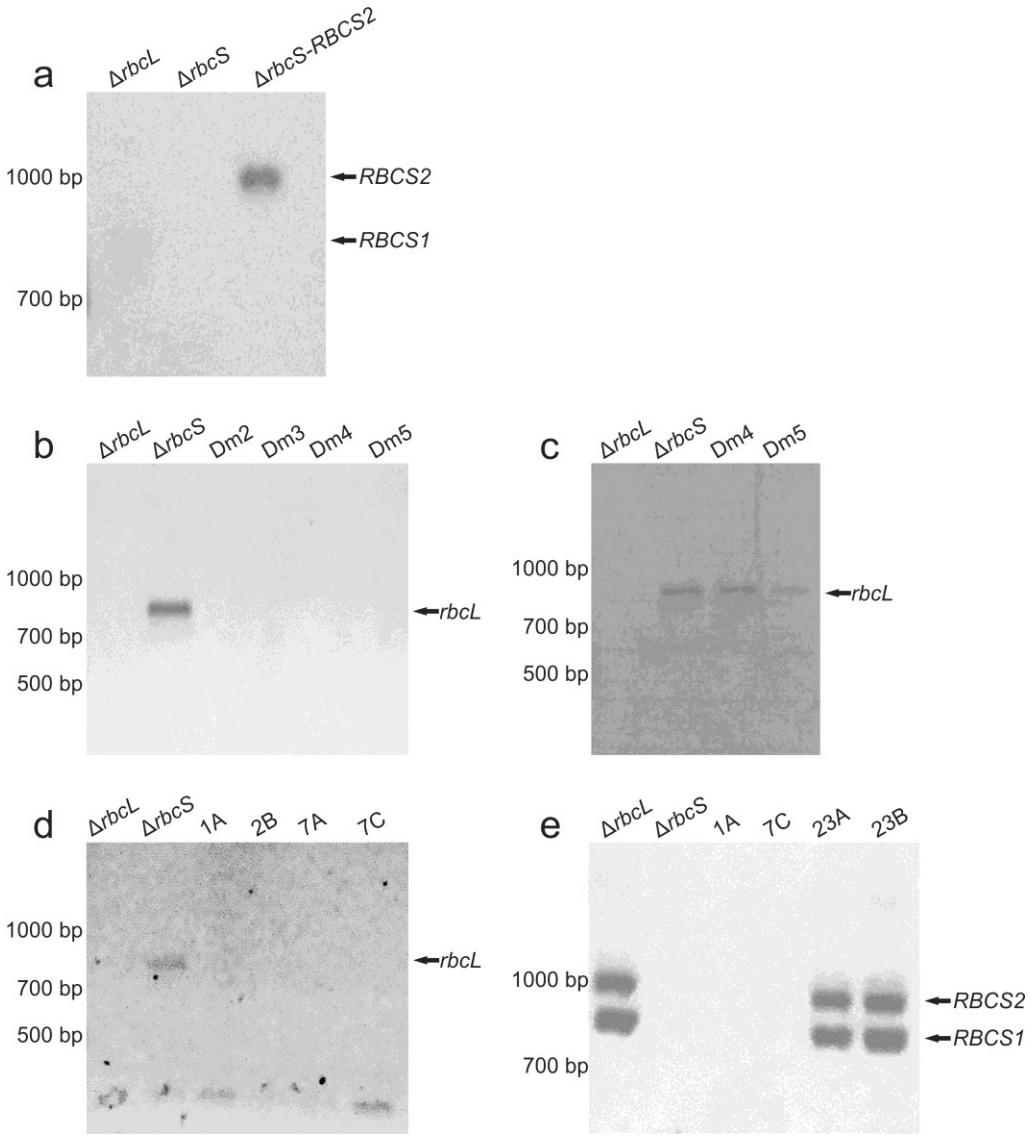

Supplementary Figure 1) PCR Analyses of mutants generated in this study.

a) Analysis of the rescued *ΔrbcS-dim1* mutant. The arrows indicate the predicted size of the PCR products from *RBCS1* and *RBCS2* (844 bp and 1019 bp, respectively). b) Analysis of double mutants obtained by chloroplast transformation. Double mutants (Dm) 2-5 initially had no detectable *rbcL* PCR product (829 bp, indicated by arrow in *ΔrbcS*). c) Analysis of double mutants obtained by chloroplast transformation following several generations without selection. *rbcL* was detectable in all transformants (shown are

Dm4 and Dm5). d) and e) Mating of *ΔrbcS* and *ΔrbcL* strains yielded double mutant progeny with no detectible *rbcL* or *RBCS* PCR products, respectively. Strain 1a was used for phenotypic analysis of the Δ*rbcL;*Δ*rbcS* genotype.

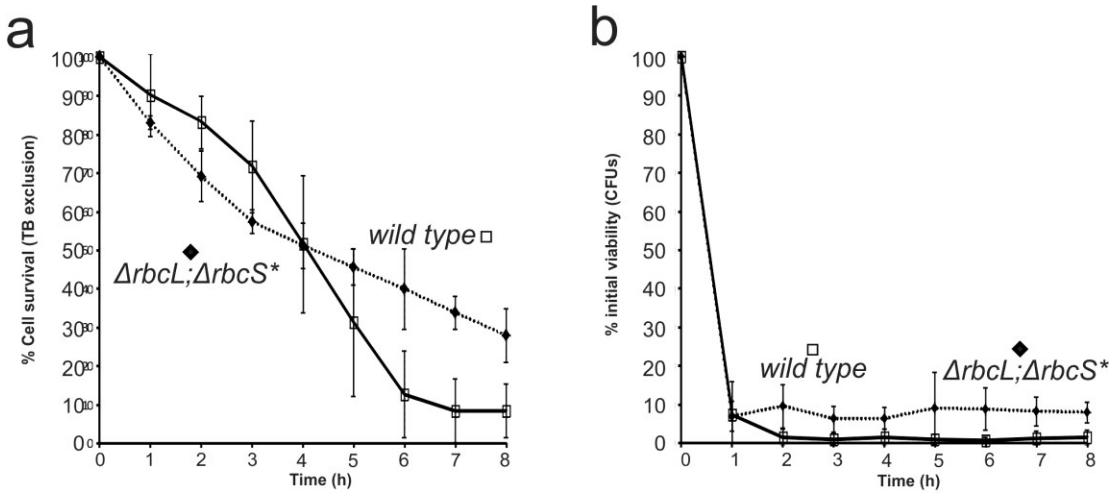

Supplementary Figure 2) Time course assays of cell survival and viability of a Δ*rbcL;*Δ*rbcS* strain that reverted back to Δ*rbcS*. The mean percentage of initial survival as measured by Trypan Blue exclusion **(**a), and the mean percentage of initial viability as measured by CFU concentration (b), in response to 4 mM H_2O_2. Error bars indicate one standard error.

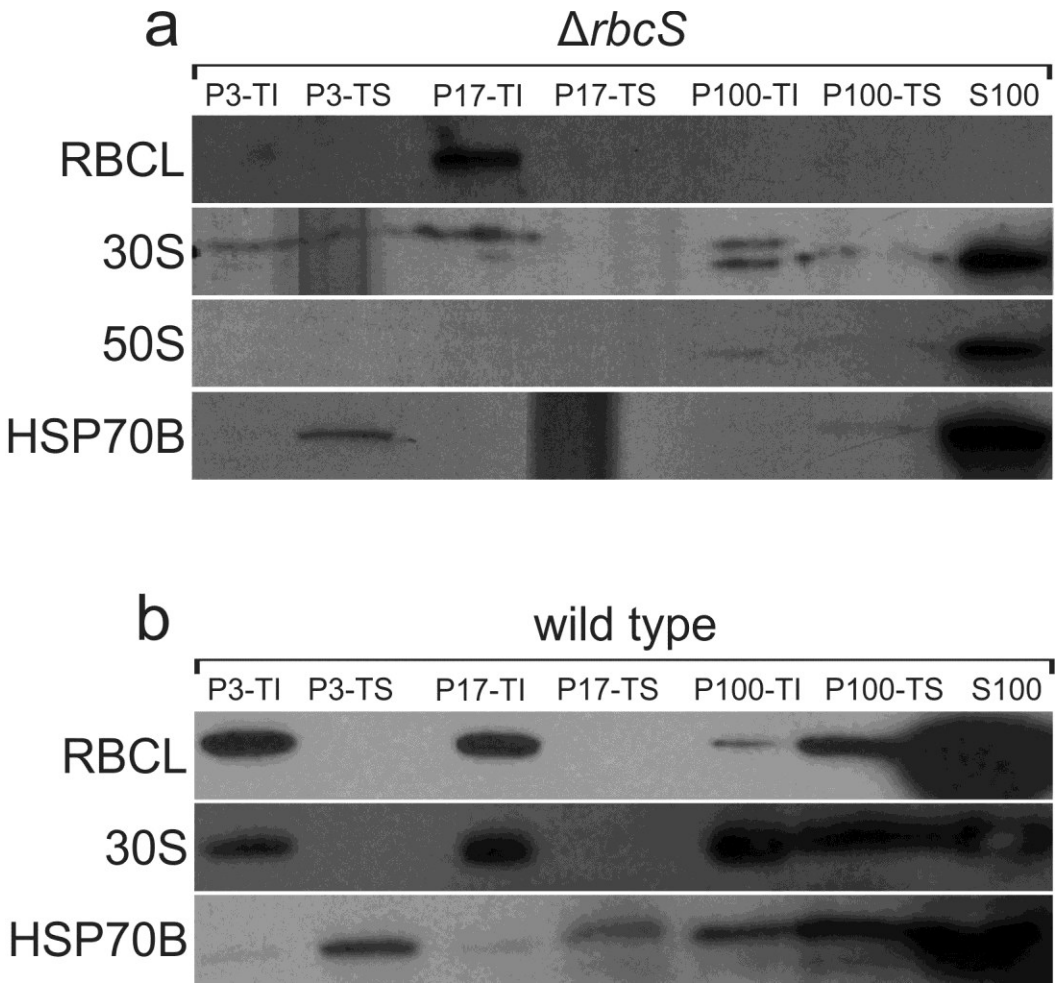

Supplementary Figure 3) Initial Differential Centrifugation Experiment. RBCL localization during differential centrifugation and differential solubilisation with Triton X-100 was revealed by immunoblot analyses for a) *ΔrbcS-dim1* and b) wild-type. Proteins analyzed were RBCL, RBCS, marker proteins for chloroplast ribosome subunits (30S and 50S), and a soluble protein of the chloroplast (HSP70B).

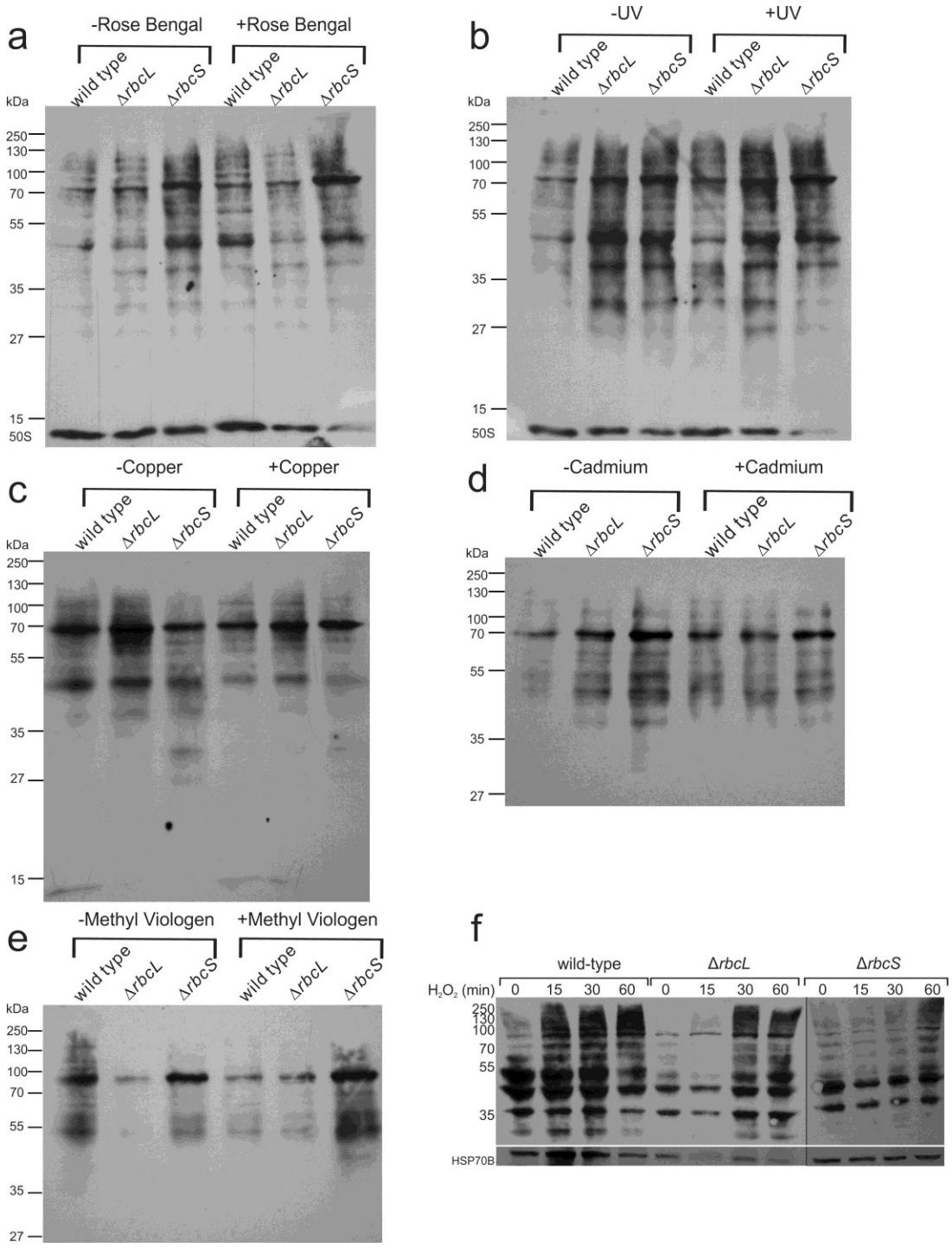

Supplementary Figure 4) Sample Oxyblot Westerns showing protein carbonylation. Oxidative damage to protein was determined as the levels of carbonylated amino acid residues by the OxyBlot kit (Millipore), in wild type, *ΔrbcL-MX3312* and *ΔrbcS-dim1*. Protein carbonylation from each strain is shown both prior to- and following treatment

with rose bengal (a), UV (b), copper (c), cadmium (d), methyl viologen (e), and H_2O_2 (f). The rose bengal and UV oxyblots were immunoprobed for a 30S protein to control for protein loading. The H_2O_2 oxyblot was immunoprobed for HSP70B to control for protein loading. Molecular weight markers are shown on the left borders of each image. Black lines indicate where immunoblots of two gels were joined, for which all detection steps were carried out in the same conditions.

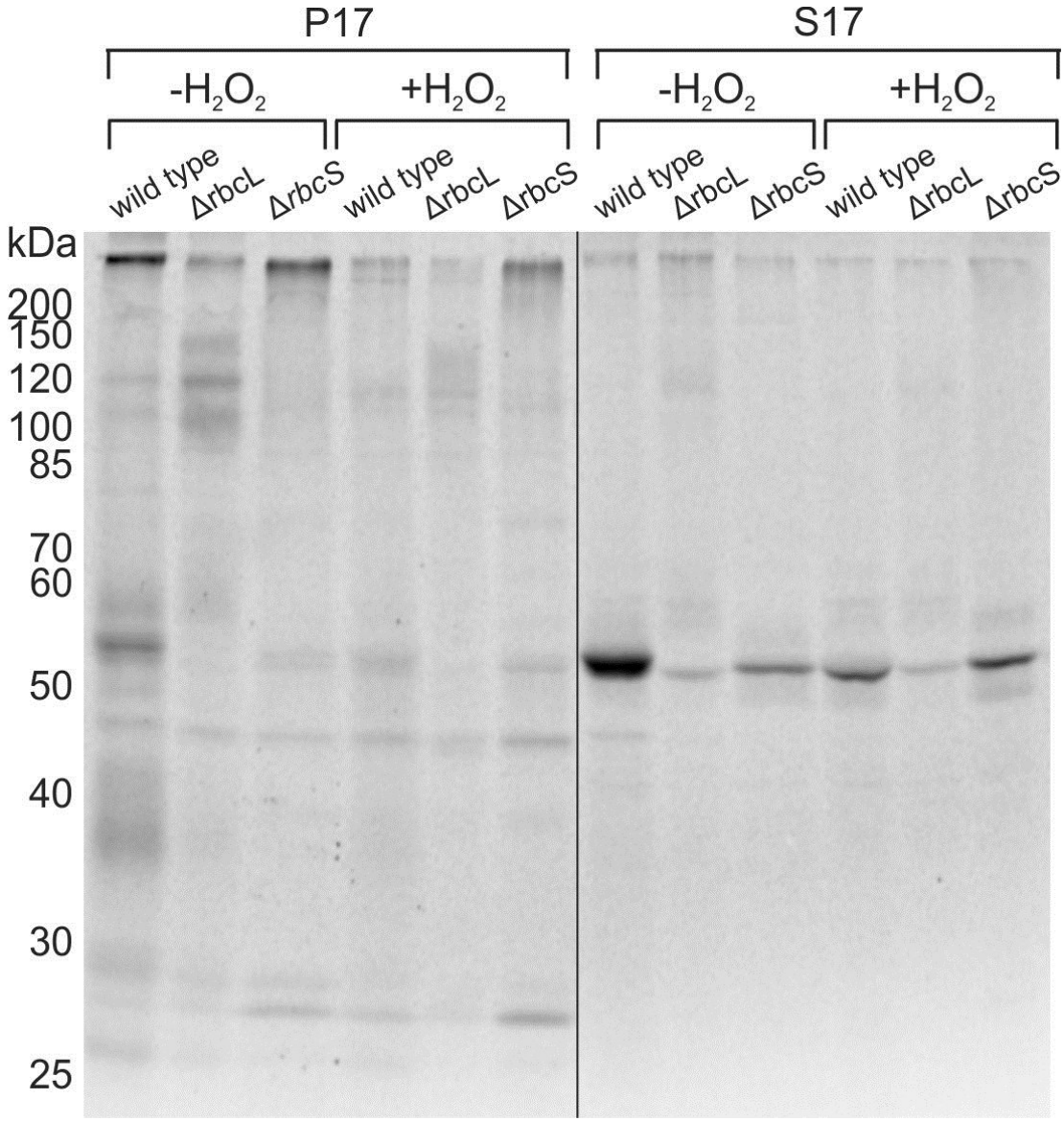

Supplementary Figure 5) ^{35}S-pulse labelling of soluble and insoluble protein. Cell lysates from wild type, *ΔrbcL-MX3312* and *ΔrbcS-dim1* strains, both prior to- and following exposure to 4 mM H_2O_2, were separated into soluble (S17) and insoluble (P17) fractions. Molecular weight markers are shown on the left border. Black lines indicate where cropped images of the same exposure were joined.